Electronic Supporting Information

Nitride Protonation and NH_3 Binding versus N–H Bond Cleavage in Uranium Nitrides

Megan Keener,[a] Rosario Scopelliti,[a] and Marinella Mazzanti*[a]

[a]Institut des Sciences et Ingénierie Chimiques, École Polytechnique Fédérale de Lausanne (EPFL), CH-1015 Lausanne, Switzerland.

*Email to whom correspondence should be addressed: mmazzanti@epfl.ch

Table of Contents

S1. Materials and Physical Measurements

General Considerations

All manipulations were performed under an atmosphere of dry, oxygen-free Ar by means of standard Schlenk or glovebox techniques (MBraun (equipped with a -40 °C freezer) glovebox). Anhydrous solvents were dried over potassium/benzophenone (THF, toluene, and diethyl ether (Et_2O)), sodium sand/benzophenone (n-hexanes), or CaH_2 for several days (pyridine) and distilled. Deuterated solvents for NMR spectroscopy were purchased from Cortecnet: d_8-THF was distilled over potassium/benzophenone and freeze-degassed, d_6-DMSO was freeze-degassed and dried over 3 Å molecular sieves for several days prior to use, and d_6-pyridine was dried over CaH_2 for several days followed by distillation and subsequent storage on activated 4 Å molecular sieves. Depleted uranium turnings were purchased from IBILABS, Florida, USA. Unless otherwise noted, reagents were purchased from commercial suppliers and used as received. $[Cs(U^{IV}(OSi(O^tBu)_3)_3)_2(\mu\text{-}N)]$ (**A**),[1] $[(U^{IV}((N(SiMe_3)_2)_2(THF))_2(\mu\text{-}N)][BPh_4]$ (**B**),[2] and $[(U^{IV}((N(SiMe_3)_2)_3(\mu\text{-}N)][NBu_4]$ (**C**)[3], $HNEt_3BPh_4$[4], and NH_4BPh_4[4] were prepared as previously described. Complexes **2-$^{14/15}$N**, and **5-$^{14/15}$N** were isotopically enriched by using $^{15}NH_4BPh_4$[4] in the initial syntheses as described below (Section S2).

Caution: *Depleted uranium (primary isotope ^{238}U) is a weak α-emitter (4.197 MeV) with a half-life of 4.47 x 10^9 years. Manipulations and reactions should be carried out in monitored fume hoods or in an inert glovebox in a radiation laboratory equipped with α- and β-counting equipment.*

Physical Measurements

NMR spectra were obtained on a AVANCENEO 400 MHz spectrometer, and referenced to residual solvent resonances of THF (d_8-THF), pyridine (d_6-pyridine), or externally (^{11}B: 85% $(Et_2O)BF_3$). All ^{11}B NMR spectra were processed using MestReNova software in order to reduce background signal with a linewidth of approximately 3000 Hz from the Pyrex NMR tubes adapted with J. Young valves. The NMR time-domain data were first left-shifted to discard the first ~0.1 ms. To correct the linear phase change, linear prediction (LP) was used to fill the initial discarded data before Fourier transform or an appropriate linear phase correction is applied to the frequency domain data after Fourier transform.

Elemental analyses were performed under an inert atmosphere of nitrogen with a ThermoScientific Flash 2000 Organic Elemental Analyzer.

X-ray crystallography data for the analysed crystal structures were collected using Cu K_α radiation on a Rigaku SuperNova dual system in combination with Atlas type CCD detector operating at T = 140.01(10) K. Single clear pale colorless irregular crystals of complex **1** (dimensions 0.12 × 0.07 × 0.06 mm^3), single colorless prism-shaped crystals of complex **2** (dimensions 0.17 × 0.10 × 0.04 mm^3), single clear light blue irregular crystals of complex **3** (dimensions 0.16 × 0.13 × 0.11 mm^3), single yellow prism crystals of complex **4** (dimensions 0.18 × 0.11 × 0.08 mm^3), single clear dark brown prism crystals of complex **4-Pyr** (dimensions 0.36 × 0.10 × 0.08 mm^3), and single clear intense orange plate crystals of complex **5** (dimensions 0.25 × 0.13 × 0.06 mm^3) were used as supplied. The following data reduction and correction were carried out by *CrysAlis^{Pro}*.[5] The solutions and refinements were performed by *SHELXT* and *SHELXL*,[6, 7] respectively. The crystal structures were refined using full-matrix least-squares based on $\boldsymbol{F^2}$ with all non-H atoms defined in anisotropic manner. Hydrogen atoms were placed in calculated positions by means of the "riding" model. The refinement of the crystal structures needed some restraints dealing with atomic distances (SADI. DFIX,

DANG cards) or anisotropic refinement (RIGU, SIMU instructions). This was due to the disorder displayed, mostly, by some ligands or solvent molecules. The raw data of **3** and **4** were treated for twinning (2 major domains were found) and the refinement was completed by using the HKLF 5 format (MERG 0, BASF = 0.4150(9) (**3**), 0.375(1) (**4**)). The disordered solvent (THF or pyridine) was removed by using the *SQUEEZE* algorithm of *PLATON*[8] during the refinement of complexes **1**, **3**, **4**, and **4-pyr**.
CCDC numbers are 2097366 (complex **1**); 2097072 (complex **2**); 2097071 (complex **3**) ; 2097368 (complex **4**); 2097367 (complex **4-pyr**); and 2097369 (complex **5**).

S2. Synthesis

Synthesis of [(U^{IV}(OSi(O^tBu)$_3$)$_3$)$_2$(μ-THF)$_2$(μ-NH)] (1): A 15 mL vial equipped with a glass-coated magnetic stirbar was charged with **A** (22.0 mg, 0.01 mmol) and 1.5 mL of THF. In a separate vial, $HNEt_3BPh_4$ (4.2 mg, 0.01 mmol, 1.0 equiv.) was dissolved in 0.3 mL of THF. Both solutions were chilled to -40°C. The solution of $HNEt_3BPh_4$ were then added dropwise to the stirring solution of **A**, where the solution went from dark red-brown to green with immediate precipitation of a white solid ($CsBPh_4$) from the reaction mixture. This was stirred at room temperature for 1 hour. Stirring was discontinued and the mixture was filtered over a 0.22 μm porosity filter frit to yield a green solution. All volatiles were removed under vacuum at room temperature yielding a microcrystalline green solid. The solid was extracted into *n*-hexanes (2 mL) and filtered over a 0.22 μm porosity filter frit to remove the remaining $CsBPh_4$. The volatiles were removed under vacuum, yielding a tan microcrystalline solid (14.2 mg, 69 % yield). Pale green single crystals suitable for XRD analysis formed over 24 hours from a concentrated THF solution of **1** kept at -40ºC. Complex **1** can also be recrystallized from a concentrated toluene solution at -40ºC. Complex **1** is soluble in all common solvents (THF, *n*-hexanes, toluene, and Et_2O). **^{1}H NMR** (400 MHz, d_8-THF, 298K): δ 0.72 (broad singlet, -OSi(O^tBu)$_3$); δ 150.3 ppm (broad singlet, -NH); (**Figure S10**). *Anal. Calcd*. for $C_{72}H_{163}NO_{24}Si_6U_2$: C, 41.74; H, 7.93: N, 0.68. *Found*: C, 42.04; H, 7.55: N, 0.77.

Isolation of [U^{IV}((OSi(O^tBu)$_3$)$_3$(THF)$_2$(NH_3)][BPh_4] (2) and [(U^{IV}(OSi(O^tBu)$_3$)$_3$(NH_3))$_2$(μ-NH_2)$_2$] (3). A 15 mL vial was charged with **A** (88.1 mg, 0.04 mmol) and dissolved in 6 mL of THF. In a separate 15 mL vial, NH_4BPh_4 (40.4 mg, 0.12 mmol, 3.0 equiv.) was added. The solution of **A** was added dropwise to the stirring, neat NH_4BPh_4, where upon addition, the solution turned teal in color with precipitation of a white solid ($CsBPh_4$). The mixture was allowed to stir for 12 hours. The mixture was filtered over a 0.22 μm porosity frit, yielding a teal solution. The volatiles were removed and the teal solid was extracted into Et_2O and filtered over a 0.22 μm porosity frit to remove the remaining $CsBPh_4$. The volatiles were removed and the solid was dissolved in minimal Et_2O (0.2 mL) and placed at -40°C. After 24 hours, two types of crystals formed; small teal plates and large teal blocks, which were analyzed by XRD analysis and identified as [U^{IV}(OSi(O^tBu)$_3$)$_3$(THF)$_2$(NH_3)][BPh_4] (**2**), and [(U^{IV}(OSi(O^tBu)$_3$)$_3$(NH_3))$_2$(μ-NH_2)$_2$] (**3**), respectively. Few large teal blocks were separated from the teal plates and analyzed by ^{1}H and ^{11}B{^{1}H} NMR spectroscopies (**Figure S9**) and were identifiable as complex **3**. Attempts to separate larger quantities of analytically pure **4** always resulted in mixtures of **2** and **3**.

Characterization of 2; **^{1}H NMR** (400 MHz, d_8-THF, 298K): δ 9.6 (broad s, OSi(O^tBu)$_3$); 5.6-5.4 (m, BPh_4); -160.1 (broad singlet, NH_3) ppm. **^{11}B** and **^{11}B{^{1}H} NMR** (128 MHz, d_8-THF, 298K): δ -8.1.

Characterization of 3; **^{1}H NMR** (400 MHz, d_8-THF, 298K): δ 4.9 (broad s, OSi(O^tBu)$_3$, 108H); -5.7 (s, OSi(O^tBu)$_3$, 54H); -10.6 (s, NH_2, 4H); -70.5 (s, NH_3, 6H) ppm (**Figure S9**).

Synthesis of [U^{IV}((OSi(O^tBu)$_3$)$_3$(THF)$_2$(NH_3)][BPh_4] (2): A 15 mL vial equipped with a glass-coated magnetic stirbar was charged with **A** (55.0 mg, 0.025 mmol) and 3 mL of THF. In a separate vial, NH_4BPh_4 (75.9 mg, 0.225 mmol, 9.0 equiv.) was dissolved in 2 mL of THF and then added dropwise to the stirring solution of **A**, resulting in a color change from dark red-brown to teal and immediate precipitation of a white solid ($CsBPh_4$). The reaction mixture was stirred at room temperature for 18 hours. Stirring was discontinued and the mixture was filtered over a porosity 4 glass fritted funnel, yielding a teal filtrate and white filter cake ($CsBPh_4$). All volatiles were removed under vacuum at room temperature yielding a microcrystalline teal solid. The solid was further triturated with *n*-hexanes (3 x 2 mL) with removal of the

volatiles each time. The solid was then extracted into a minimal amount of *n*-hexanes (4 mL) and filtered over a 0.22 μm porosity filter frit in which the volatiles were removed under vacuum. The solid was then extracted into a minimal amount of Et_2O (2 mL), filtered over an additional 0.22 μm porosity filter frit and the volatiles removed, yielding a teal microcrystalline solid with complete separation from $CsBPh_4$ (61.7 mg, 82 % yield). Single crystals suitable for XRD analysis formed over 24 hours from a concentrated ethereal solution of **2** at -40ºC. Complex **2** is soluble in all common solvents (THF, *n*-hexanes, and Et_2O). **^{1}H NMR** (400 MHz, d_8-THF, 298K): δ 9.6 (broad s, $OSi(O^tBu)_3$); 5.6-5.4 (m, BPh_4); -160.1 (broad singlet, NH_3) ppm (**Figure S8**). **^{11}B** and **^{11}B{^{1}H} NMR** (128 MHz, d_8-THF, 298K): δ -8.1 (**Figure S8**). *Anal. Calcd*. for $C_{60}H_{104}NO_{12}Si_3BU$: C, 52.81; H, 7.68: N, 1.03. *Found*: C, 52.64; H, 7.59: N, 1.02.

General synthesis of $[(U^{IV}(THF)_4)_2(\mu\text{-}N)(\mu\text{-}NH_2)_2][BPh_4]_3$ (5) from complexes B, E, or C. A 15 mL vial was charged with nitride complex **B**, **E**, or **C** (0.07 mmol) and 3 mL of THF. In a separate vial, NH_4BPh_4 (2.2-4.2 equiv.) was dissolved in 2 mL of THF and then added in one portion to the solution of the nitride complex where the solution went from dark red-brown to golden yellow. Within 30 minutes, golden crystalline solid began to precipitate, and this was allowed to react at room temperature for 12 hours. The solid was collected over a porosity 4 fritted filter and washed with THF (3 x 2 mL) to yield crystalline **5** (83-89 % yield). Single crystals suitable for XRD analysis were grown from a small-scale reaction (0.0035 mmol of the nitride complex) in dilute THF (4 mL) at room temperature. Complex **5** is soluble in pyridine and insoluble in most common solvents (THF, *n*-hexanes, toluene, and Et_2O). **^{1}H NMR** (400 MHz, d_5-pyridine, 298K): δ 7.3-6.2 (s, BPh_4); -468 (broad s, NH_2) ppm (**Figure S21**). **^{11}B** and **^{11}B{^{1}H} NMR** (128 MHz, d_8-THF, 298K): δ -7.9 (**Figure S21**).
Quantities from synthesis with complex B: **B** (111.7 mg, 0.07 mmol); NH_4BPh_4 (51.9 mg, 0.154 mmol, 2.2 equv.). Yield of **5** (119.4 mg, 83 % yield).
Quantities from synthesis with complex E: **E** (84.2 mg, 0.07 mmol); NH_4BPh_4 (75.5 mg, 0.224 mmol, 3.2 equiv.). Yield of **5** (128.1 mg, 89 % yield).
Quantities from synthesis with complex C: **C** (124.0 mg, 0.07 mmol); NH_4BPh_4 (99.2 mg, 0.294 mmol, 4.2 equiv.). Yield of **5** (103.6 mg, 72 % yield).
Anal. Calcd. for $C_{92}H_{104}N_3O_5B_3U_2$: C, 60.04; H, 5.70: N, 2.28. *Found*: C, 59.93; H, 5.867: N, 2.01.

S3. Reactivity studies

S3.1. Reactivity of $OSi(O^tBu)_3$-complex, A.

Reaction of A with 1.0 equiv. NH_4BPh_4. A 1 mL vial was charged with **A** (7.7 mg, 0.0035 mmol) and dissolved in 0.5 mL of d_8-THF. In a separate 1 mL vial, NH_4BPh_4 (1.2 mg, 0.0035 mmol, 1.0 equiv.) was added. Both vials were chilled to -40°C. The chilled solution of **A** was added in a single portion to the solution of NH_4BPh_4, where upon addition the solution turned green-blue in color with precipitation of a white solid ($CsBPh_4$). The mixture was transferred to a prechilled NMR tube equipped with a J-Young valve and the solution was analyzed by ^{1}H NMR spectroscopy (**Figure S1**), resulting in unreacted complex **A**, formation of **1** and **2**, as well as multiple unidentifiable species.

Reaction of A with 3.0 equiv. NH_4BPh_4; *in-situ* identification and isolation of complexes 2 and 3. A 1 mL vial was charged with **A** (7.7 mg, 0.0035 mmol) and dissolved in 0.5 mL of d_8-THF. In a separate 1 mL vial, NH_4BPh_4 (3.5 mg, 0.0105 mmol, 3.0 equiv.) was added. The solution of **A** was added in a single portion to the neat NH_4BPh_4, where upon addition, the solution turned teal in color with contaminant

precipitation of a white solid ($CsBPh_4$). The mixture was transferred to a NMR tube equipped with a J-Young valve and the solution was analyzed by ^{1}H NMR spectroscopy (**Figure S2**), where the evolution of complexes **2** and **3** were monitored over 4 days resulting in no change in the following spectra.
Identification of 2; **^{1}H NMR** (400 MHz, d_8-THF, 298K): δ 9.6 (broad s, $OSi(O^tBu)_3$); 5.6-5.4 (m, BPh_4); -160.1 (broad singlet, NH_3) ppm.
Identification of 3; **^{1}H NMR** (400 MHz, d_8-THF, 298K): δ 4.9 (broad s, $OSi(O^tBu)_3$, 108H); -5.7 (s, $OSi(O^tBu)_3$, 54H); -10.6 (s, NH_2, 4H); -70.5 (s, NH_3, 6H) ppm.

Reaction of A with 3.0-9.0 equiv. NH_4BPh_4. Addition of (3.0-9.0 equivalents) NH_4BPh_4 to a solution of **A** in d_8-THF resulted in the appearance of multiple new resonances in the ^{1}H NMR spectrum attributable to two independent species, as the relative integration of the signal at δ 9.6 ppm increased compared to the signal at δ 5.1 ppm (roughly 15-fold) upon addition of excess (9.0 equiv.) NH_4BPh_4 (**Figure S3**). Direct addition of 9.0 equiv. of NH_4BPh_4 to **A**, resulted in the clean formation of one single product as indicated by ^{1}H NMR spectroscopy (**Figure S4**).
3.0 equiv. total: A 1 mL vial was charged with **A** (7.7 mg, 0.0035 mmol) and dissolved in 0.5 mL of d_8-THF. In a separate 1 mL vial, NH_4BPh_4 (3.5 mg, 0.0105 mmol, 3.0 equiv.) was added. The solution of **A** was added in a single portion to the neat NH_4BPh_4, where upon addition, the solution turned teal in color with contaminant precipitation of a white solid ($CsBPh_4$). The mixture was allowed to react for 6 hours and transferred to a NMR tube equipped with a J-Young valve and the solution was analyzed by ^{1}H NMR spectroscopy (**Figure S2** and a, **Figure S3**), resulting in formation of complexes **2** and **3**.
6.0 equiv. total: A separate 1 mL vial was charged with NH_4BPh_4 (3.5 mg, 0.0105 mmol, 3.0 equiv.), where the NMR sample generated above (3.0 equiv. total), was added in a single portion to the neat NH_4BPh_4. The mixture remained teal with precipitation of the white solid. This was allowed to react for 6 hours and was analyzed by ^{1}H NMR spectroscopy (b, **Figure S3**), resulting in higher quantity of **2** and decrease of **3**.
9.0 equiv. total: A separate 1 mL vial was charged with NH_4BPh_4 (3.5 mg, 0.0105 mmol, 3.0 equiv.), where the NMR sample generated above (6.0 equiv. total), was added in a single portion to the neat NH_4BPh_4. The mixture remained teal with precipitation of the white solid. This was allowed to react for 6 hours and was analyzed by ^{1}H NMR spectroscopy (c, **Figure S3**), resulting in complex **2** as the primary species.

Reaction of A with 9.0 equiv. NH_4BPh_4; *in-situ* identification of complex 2. A 1 mL vial was charged with **A** (7.7 mg, 0.0035 mmol) and dissolved in 0.5 mL of d_8-THF. In a separate 1 mL vial, NH_4BPh_4 (10.6 mg, 0.0315 mmol, 9.0 equiv.) was added. The solution of **A** was added in a single portion to the neat NH_4BPh_4, where upon addition, the solution turned teal in color with contaminant precipitation of a white solid ($CsBPh_4$). The mixture was transferred to a NMR tube equipped with a J-Young valve and the solution was analyzed by ^{1}H NMR spectroscopy (**Figure S4**) and monitored over 12 hours, resulting in formation of complex **2** as the main species.
^{1}H NMR (400 MHz, d_8-THF, 298K): δ 9.6 (broad s, $OSi(O^tBu)_3$); 5.6-5.4 (m, BPh_4); -160.1 (broad singlet, NH_3) ppm.

Reaction of A with 1.0 equiv. $HNEt_3BPh_4$; *in-situ* identification of complex 1. A 1 mL vial was charged with **A** (7.7 mg, 0.0035 mmol) and dissolved in 0.5 mL of d_8-THF. In a separate 1 mL vial, $HNEt_3BPh_4$ (1.5 mg, 0.0035 mmol, 1.0 equiv.) was added. Both vials were chilled to -40°C. The chilled solution of **A**

was added in a single portion to the neat $HNEt_3BPh_4$, where upon addition the solution turned green in color with precipitation of a white solid ($CsBPh_4$). The mixture was transferred to a prechilled NMR tube equipped with a J-Young valve and the solution was analyzed by ^1H and $^{11}B\{^1H\}$ NMR spectroscopies (**Figure S5**), identifying **1** as the main species.
^{1}H NMR (400 MHz, d_8-THF, 298K): δ 0.72 (broad singlet, -OSi(O^tBu)$_3$); 0.98 (s, NEt_3); 2.50 (s, NEt_3) 5.6-5.4 (m, BPh_4); δ 150.3 ppm (broad singlet, -NH). **$^{11}B\{^1H\}$ NMR** (128 MHz, d_8-THF, 298K): δ -7.9 ppm.

Reaction of A with 10.0 equiv. $HNEt_3BPh_4$. A 1 mL vial was charged with **A** (7.7 mg, 0.0035 mmol) and dissolved in 0.5 mL of d_8-THF. In a separate 1 mL vial, $HNEt_3BPh_4$ (14.7 mg, 0.035 mmol, 10.0 equiv.) was added. Both vials were chilled to -40°C. The chilled solution of **A** was added in a single portion to the neat $HNEt_3BPh_4$, where upon addition the solution turned green in color with precipitation of a white solid ($CsBPh_4$). The mixture was transferred to a prechilled NMR tube equipped with a J-Young valve and the solution was analyzed by ^1H NMR spectroscopy. The mixture was brought to room temperature and monitored over the course of 8 days with stirring (**Figure S6**), resulting in a color change from green to blue. The consumption of **1** and the formation of complex **2** was identified as the main species. The yield of complex **2** was determined by integration (with an internal standard, naphthalene) of the ^1H NMR signals to be 40 %.

Control reaction of 2 with 10 equiv. $HNEt_3BPh_4$. A 1 mL vial was charged with **2** (5.3 mg, 0.0035 mmol) and dissolved in 0.5 mL of d_8-THF. In a separate 1 mL vial, $HNEt_3BPh_4$ (14.7 mg, 0.035 mmol, 10.0 equiv.) was added. Both vials were chilled to -40°C. The chilled solution of **2** was added in a single portion to the neat $HNEt_3BPh_4$, where upon addition the solution remained blue in color. The mixture was transferred to a prechilled NMR tube equipped with a J-Young valve and the solution was brought up to room temperature and analyzed by ^1H NMR spectroscopy over the course of 12 hours (**Figure S7**). The disappearance of the -NH_3 resonance at δ -160.1 ppm in complex **2** is most likely attributable to the excess $HNEt_3BPh_4$ in solution.

S3.2. Reactivity of $N(SiMe_3)_2$-complex, B.

Reaction of B with 2.0 equiv. $^{13}CO_2$. In an argon filled glovebox, a NMR tube equipped with a J-Young valve was charged with **B** (5.6 mg, 0.0035 mmol) and dissolved in 0.4 mL of d_8-THF. The tube was brought out of the glovebox, attached to a Schlenk line, and degassed by three freeze-pump-thaw cycles. To the solution, $^{13}CO_2$ (2.0 equiv. condensed) was added with an immediate color change from brown to yellow. The mixture was analyzed by ^1H NMR spectroscopy (**Figure S11**). Attempts to isolate the reaction products from the reaction mixture were not successful. The volatiles from the reaction mixture were removed and the residue was taken out of the glovebox and hydrolyzed with 0.5 mL of D_2O (pD = 12) and the hydrolysis products were analyzed by ^{13}C NMR spectroscopy with d_6-DMSO (1 drop) utilized as an internal reference (**Figure S12**).
^{13}C NMR (151 MHz, d_8-THF, 298K): δ 170.1 (s, unknown); 130.2 (s, $N^{13}CO^-$); 3.4 ppm (s, unknown).

Reaction of B with 2.0 equiv. ^{13}CO. In an argon filled glovebox, a NMR tube equipped with a J-Young valve was charged with **B** (5.6 mg, 0.0035 mmol) and dissolved in 0.4 mL of d_8-THF. The tube was brought out of the glovebox, attached to a Schlenk line, and degassed by three freeze-pump-thaw cycles. To the solution, ^{13}CO (2.0 equiv.) was added with an immediate color change from brown to yellow. The mixture

was analyzed by ^{1}H NMR spectroscopies (**Figure S13**). Attempts to isolate the reaction products were not successful. The solution was then brought back into the glovebox, and the volatiles were removed. The residue was taken out of the glovebox and hydrolyzed with 0.5 mL of D_2O (pD = 12) and the hydrolysis products were analyzed by ^{13}C NMR spectroscopy with d_6-DMSO (1 drop) utilized as an internal reference (**Figure S14**).
^{13}C NMR (151 MHz, d_8-THF, 298K): δ 166.3 (s, $^{13}CN^-$); 137.2 (s, unknown); 128.5 (s, unknown); 124.8 (s, unknown); 3.4 (s, unknown).

Reaction of B with excess H_2. In an argon filled glovebox, a NMR tube equipped with a J-Young valve was charged with **B** (5.6 mg, 0.0035 mmol) and dissolved in 0.4 mL of d_8-THF. The tube was brought out of the glovebox, attached to a Schlenk line, and degassed by three freeze-pump-thaw cycles. To the solution, H_2 (excess, 1 atm) was added and the mixture was analyzed by ^{1}H NMR spectroscopy (**Figure S15**). The solution was monitored for several days, but there was no reactivity observed.

Reaction of B with 4.0 equiv. $HNEt_3BPh_4$. A 1 mL vial was charged with **B** (5.6 mg, 0.0035 mmol) and dissolved in 0.5 mL of d_8-THF. In a separate 1 mL vial, $HNEt_3BPh_4$ (5.9 mg, 0.014 mmol, 4.0 equiv.) was added. The solution of **B** was added in a single portion to the neat $HNEt_3BPh_4$, where upon addition the solution remained brown in color with no observed color change. The mixture was transferred to a NMR tube equipped with a J-Young valve and the solution was analyzed by ^{1}H NMR spectroscopy. The mixture was monitored over the course of 2 days (**Figure S16**), resulting in unreacted **B** and $HNEt_3BPh_4$.

Reaction of B with 2.0 equiv. NH_4BPh_4; *in-situ* identification and isolation of complex 5. A 1 mL vial was charged with **B** (5.6 mg, 0.0035 mmol) and dissolved in 0.5 mL of d_8-THF. In a separate 1 mL vial, NH_4BPh_4 (2.4 mg, 0.007 mmol, 2.0 equiv.) was added. The solution of **B** was added in a single portion to the neat NH_4BPh_4, where upon addition, the solution turned yellow in color. The mixture was transferred to a NMR tube equipped with a J-Young valve and the solution was analyzed by ^{1}H NMR spectroscopy over 12 hours (**Figure S19**). Golden crystals suitable for XRD analysis were obtained from the reaction mixture at -40ºC, yielding $[(U^{IV}(THF)_4)_2(\mu\text{-}N)(\mu\text{-}NH_2)_2][BPh_4]_3$, (**5**).

Reaction of B with 1.0 equiv. NH_4BPh_4; *in-situ* identification and isolation of complex 7. A 1 mL vial was charged with **B** (5.6 mg, 0.0035 mmol) and dissolved in 0.5 mL of d_8-THF. In a separate 1 mL vial, NH_4BPh_4 (1.2 mg, 0.0035 mmol, 1.0 equiv.) was added. The solution of **B** was added in a single portion to the neat NH_4BPh_4, where upon addition, the solution turned yellow in color. The mixture was transferred to a NMR tube equipped with a J-Young valve and the solution was analyzed by ^{1}H NMR spectroscopy over 12 hours (**Figure S17**). Golden crystals suitable for XRD analysis were obtained from the reaction mixture at -40ºC, yielding $[(U^{IV}((N(SiMe_3)_2)(THF)_3)_2(\mu\text{-}NH)_2][BPh_4]_2$, (**7**). The crystals were isolated and analyzed by ^{1}H NMR spectroscopy in d_5-pyridine (**Figure S18**).
^{1}H NMR (400 MHz, d_5-pyridine, 298K): δ 7.3-6.2 (s, BPh_4); -468 (broad s, NH_2) ppm.

S4. General procedure for NH_3 formation from addition of HCl (Et_2O)

A NMR tube equipped with a J-Young valve was charged with complexes **2**, **2-$^{14/15}$N**, **5**, or **5-$^{14/15}$N** (0.007 mmol). An excess of a 1 M solution of HCl in Et_2O (0.5 mL, 0.5 mmol, 70 equiv.) was added. The reaction mixture immediately turned colorless with precipitation of solids. After 1 hour, the solvent was removed under vacuum for 3 hours, d_6-DMSO was added, and the amount of ammonia was evaluated by quantitative ^{1}H NMR spectroscopy (5.0 equiv. Me_2SO_2 as internal standard, 120s relaxation delay) (**Figure S22**) and (**Figure S23**), respectively.

S5. Supplementary Figures for NMR Spectroscopy

S5.1. NMR spectra for protonation studies with complex, A.

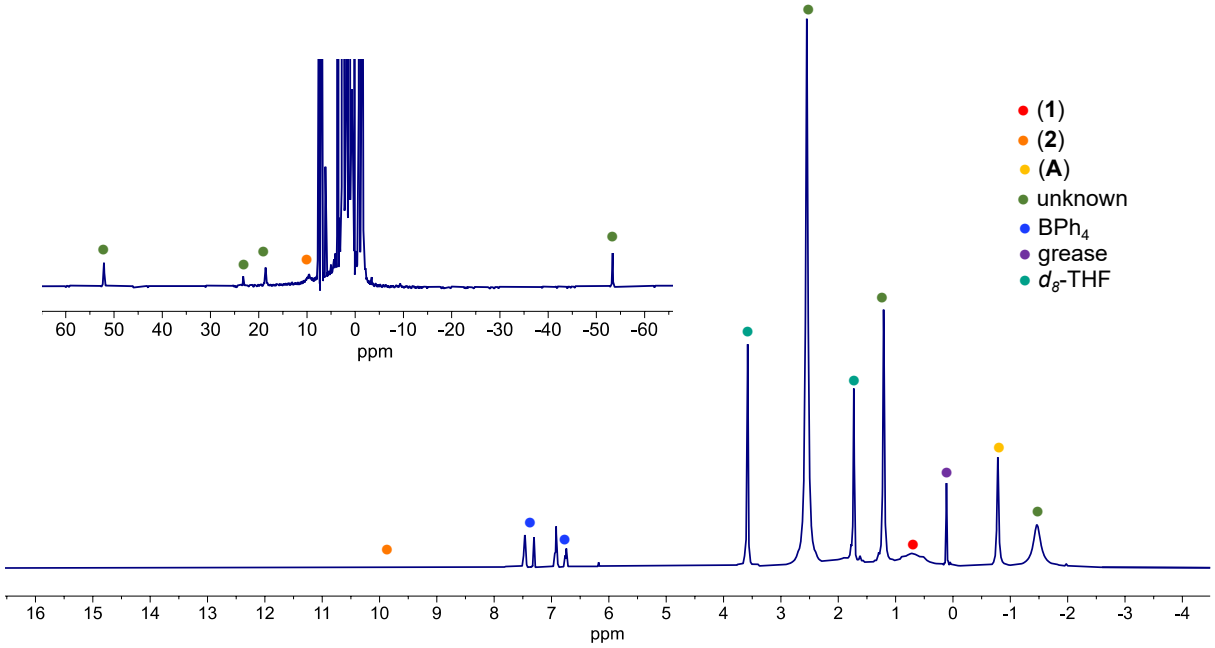

Figure S1. ^{1}H NMR (400 MHz, d_8-THF, 298K) spectra of **A** in the presence of 1.0 equiv. NH_4BPh_4.

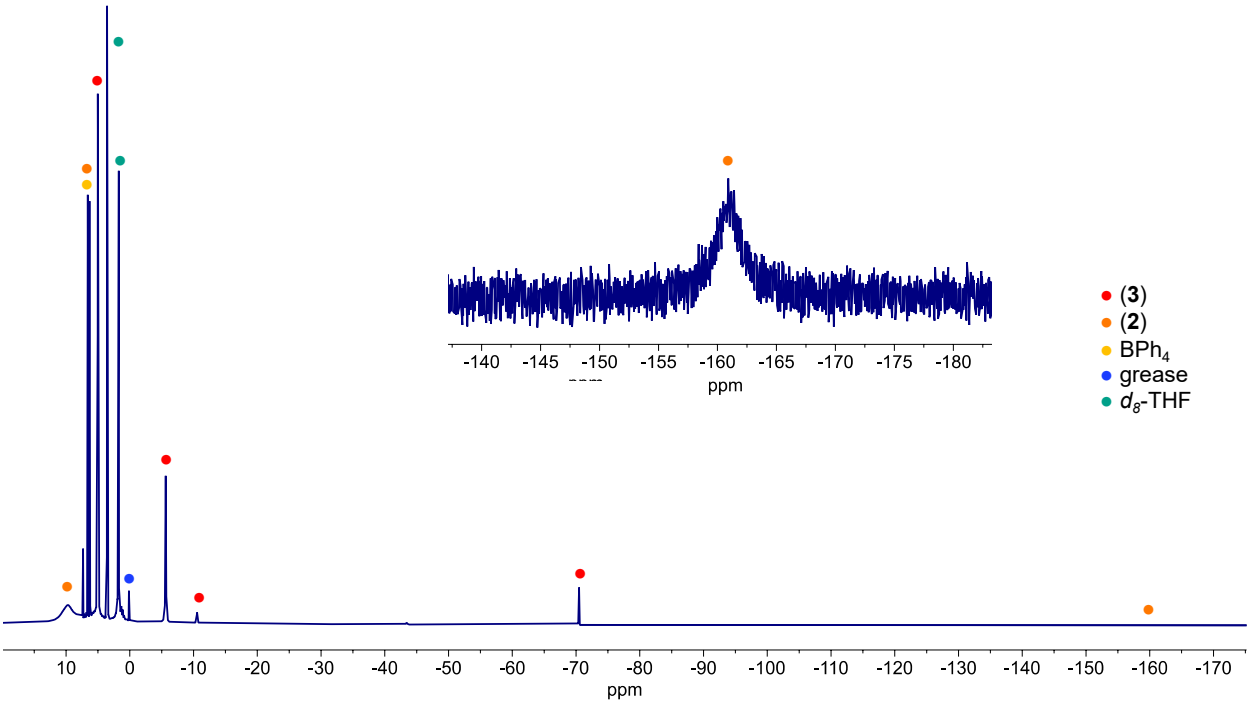

Figure S2. ^{1}H NMR (400 MHz, d_8-THF, 298K) spectra of **A** in the presence of 3.0 equiv. NH_4BPh_4, forming a mixture of complexes **2** and **3**.

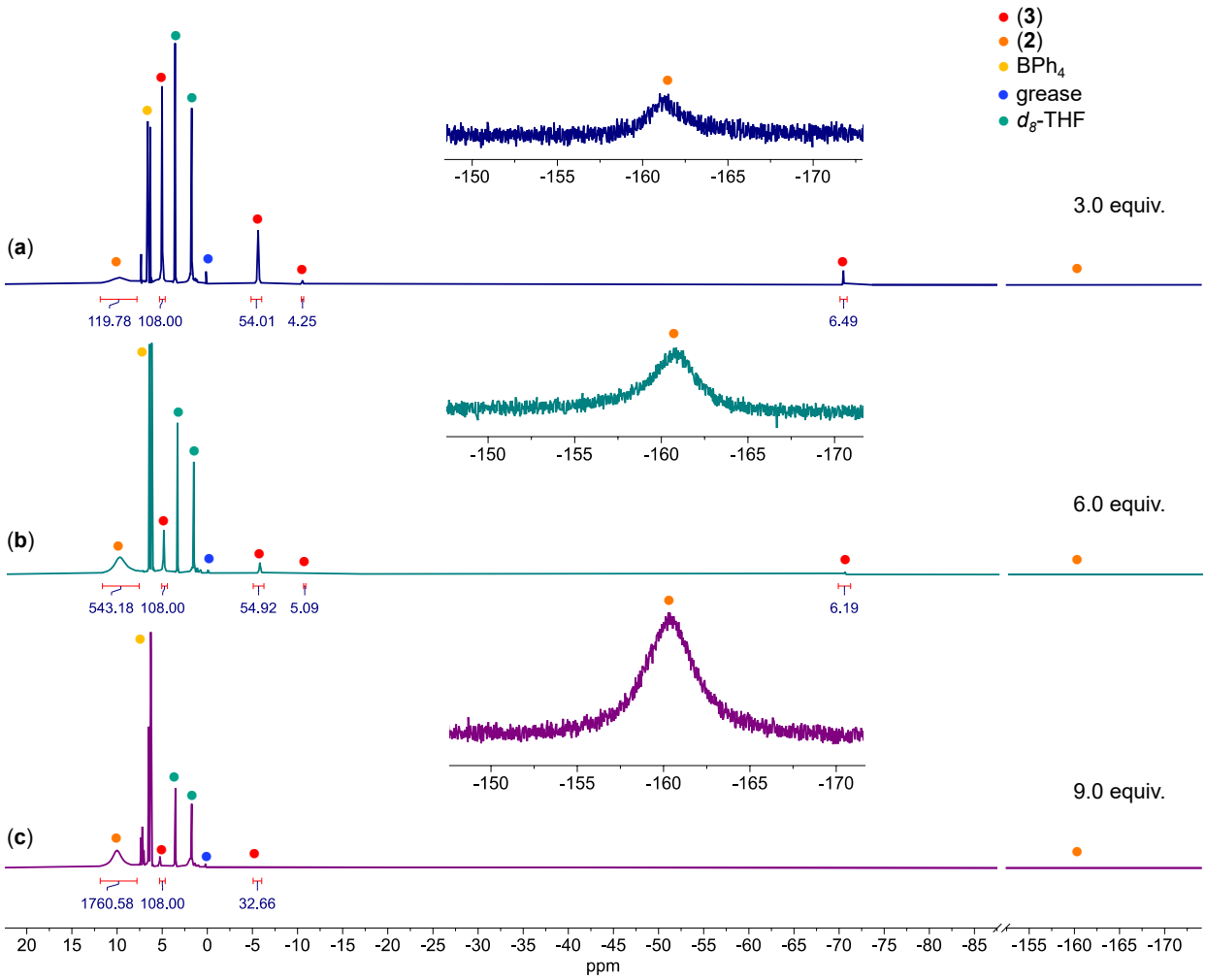

Figure S3. ^{1}H NMR (400 MHz, d_8-THF, 298K) spectra from titration experiments of **A** and NH_4BPh_4. (**a**) ^{1}H NMR (400 MHz, d_8-THF, 298K) spectrum of 1.0 equiv. **A** and 3.0 equiv. NH_4BPh_4 in d_8-THF. (**b**) ^{1}H NMR (400 MHz, d_8-THF, 298K) spectrum of 3.0 equiv. NH_4BPh_4 (6.0 equiv. total) added to the reaction in (**a**). (**c**) ^{1}H NMR (400 MHz, d_8-THF, 298K) spectrum of 3.0 equiv. NH_4BPh_4 (9.0 equiv. total) added to the reaction in (**b**).

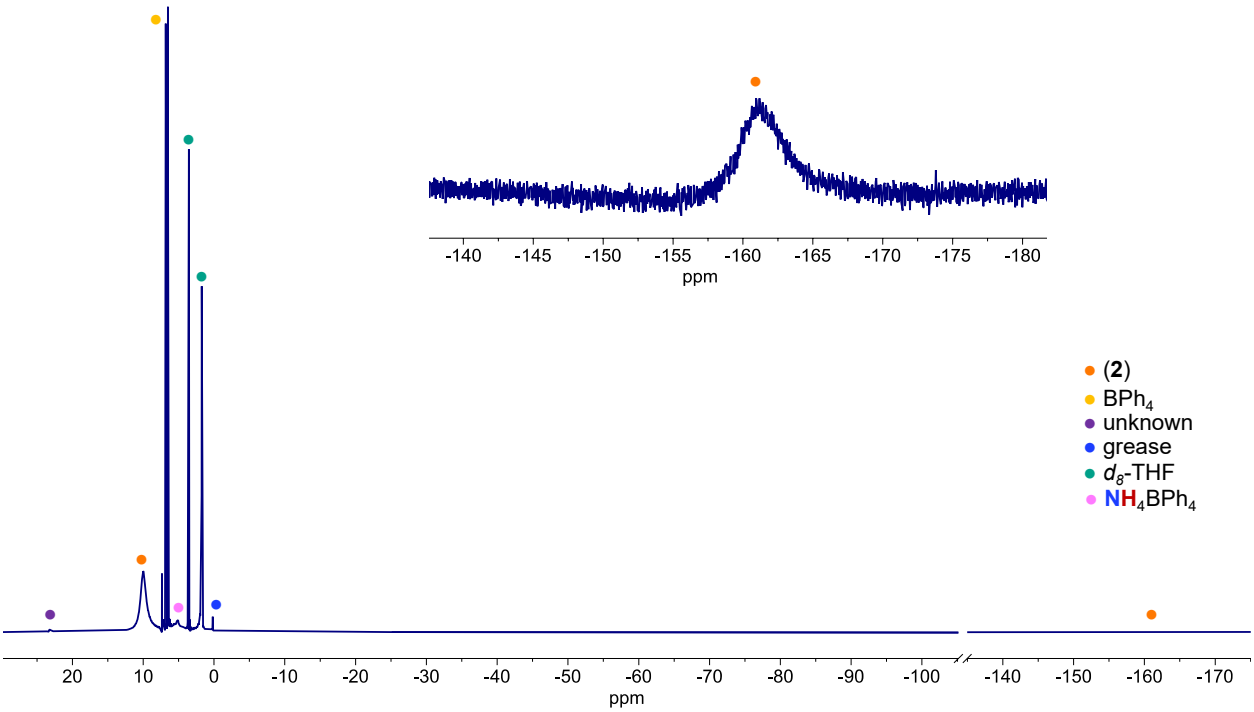

Figure S4. ^{1}H NMR (400 MHz, d_8-THF, 298K) spectra of **A** in the presence of 9.0 equiv. NH_4BPh_4, forming complex **2**.

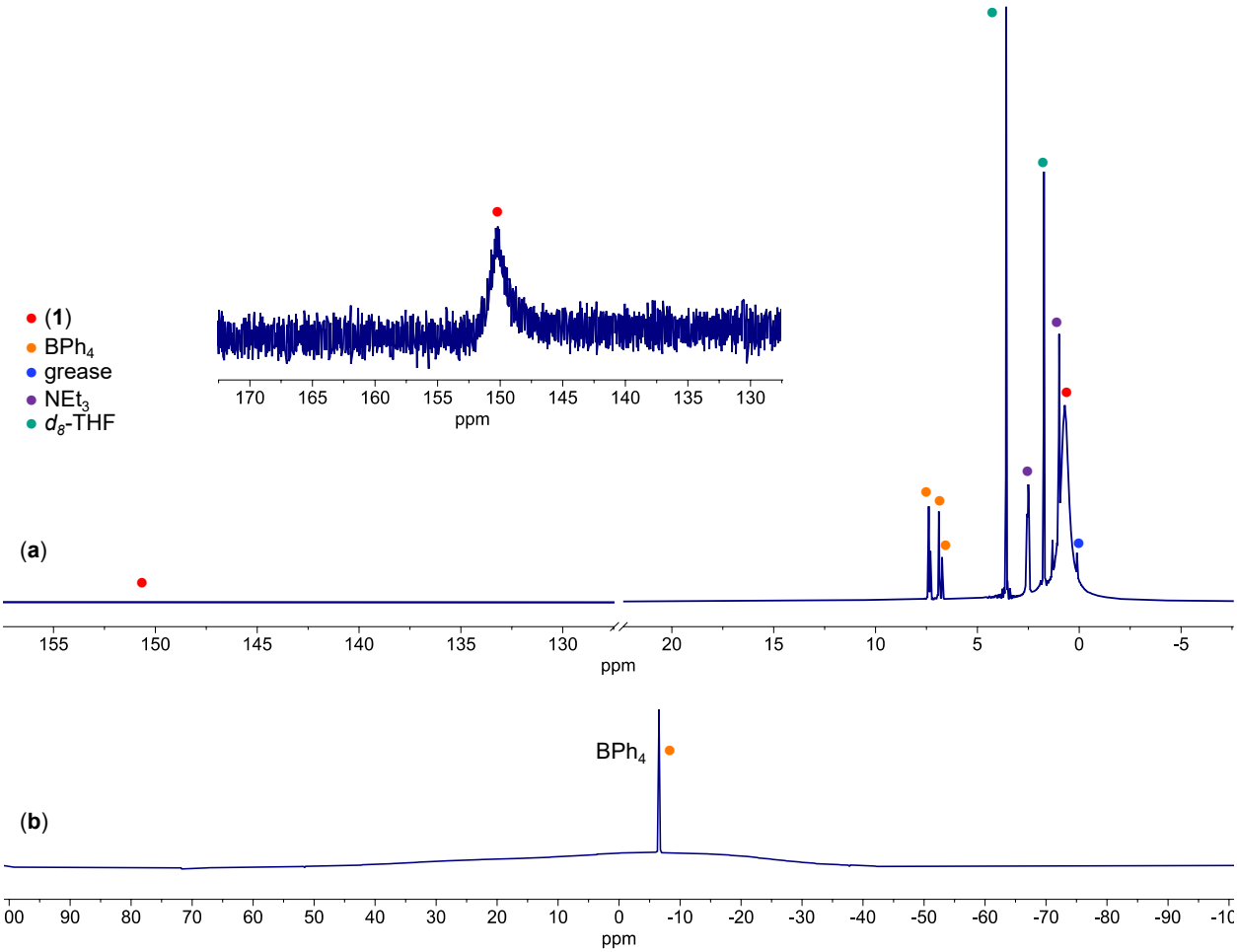

Figure S5. (**a**) ^{1}H NMR (400 MHz, d_8-THF, 298K) spectrum of **A** in the presence of 1.0 equiv. $HNEt_3BPh_4$, forming complex **1**. (**b**) $^{11}B\{^{1}H\}$ NMR (128 MHz, d_8-THF, 298K) spectrum of **A** in the presence of 1.0 equiv. $HNEt_3BPh_4$.

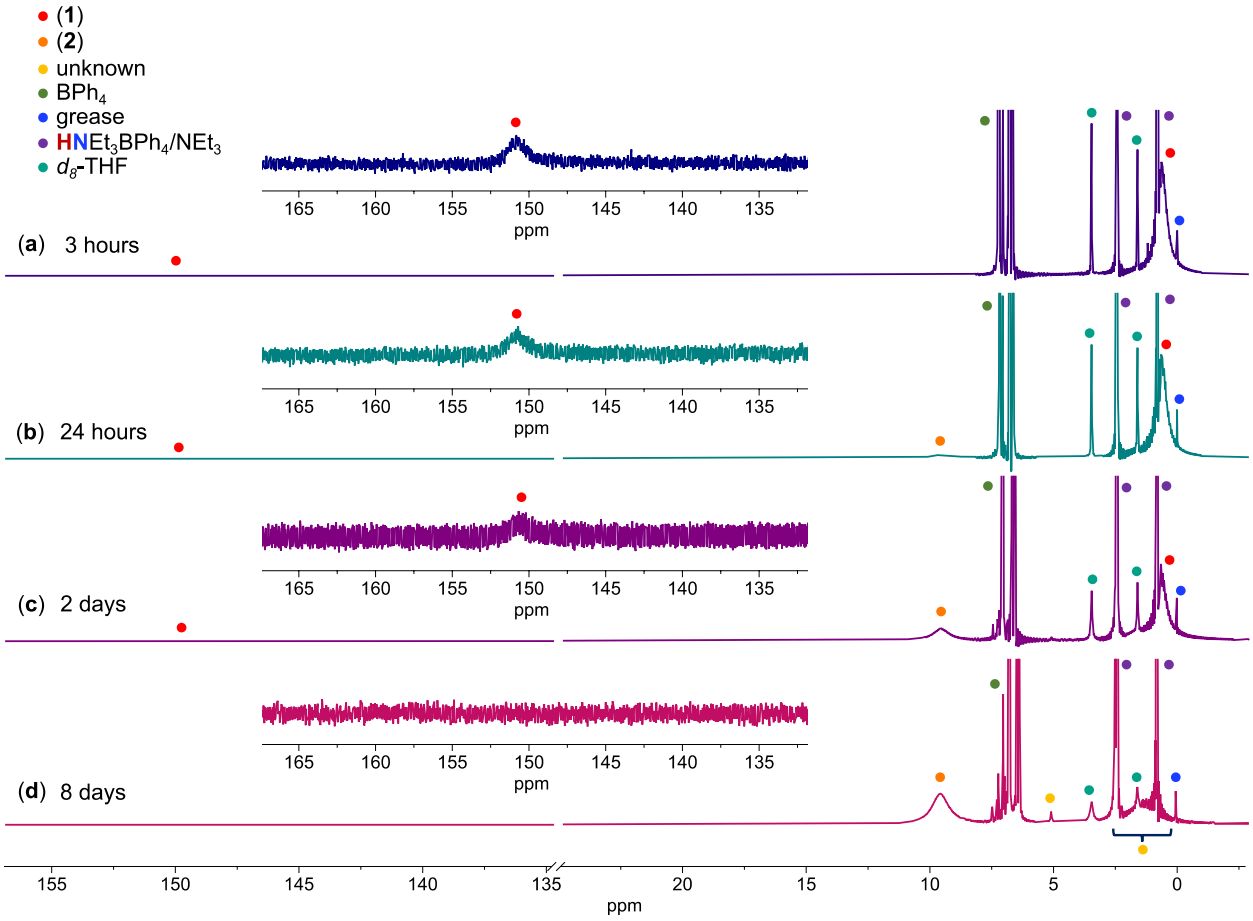

Figure S6. ^{1}H NMR (400 MHz, d_8-THF, 298K) spectra of **A** in the presence of 10.0 equiv. $HNEt_3BPh_4$ after (**a**) 3 hours (**b**) 24 hours (**c**) 2 days (**d**) 8 days.

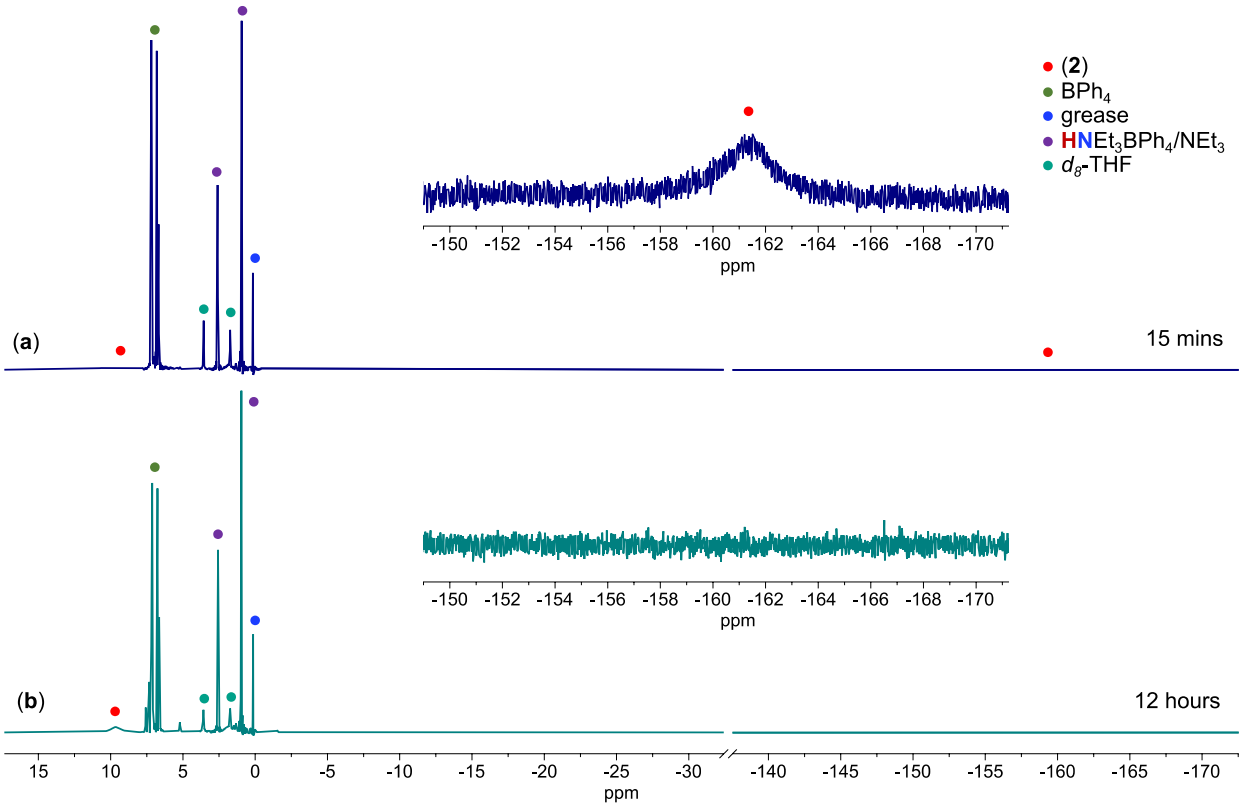

Figure S7. ^{1}H NMR (400 MHz, d_8-THF, 298K) spectra for the control reaction of **2** in the presence of 10.0 equiv. $HNEt_3BPh_4$ after (**a**) 15 mins and (**b**) 12 hours.

S5.2. NMR spectra for isolated OSi(O^{t}Bu)$_3$-containing complexes.

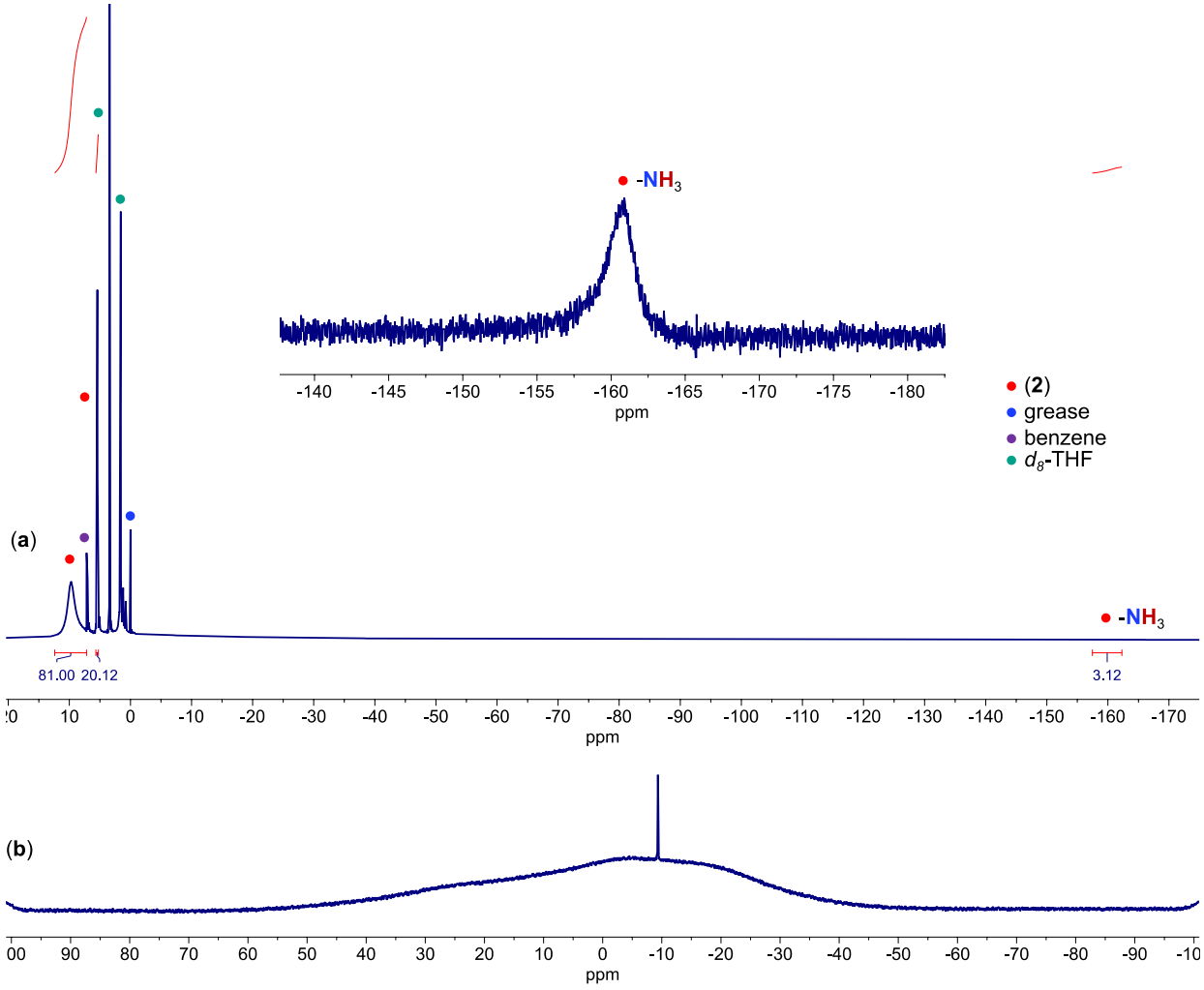

Figure S8. (**a**) ^{1}H NMR (400 MHz, d_8-THF, 298K) spectrum of [U^{IV}(OSi(O^{t}Bu)$_3$)$_3$(THF)$_2$(NH$_3$)][BPh$_4$], **2**. (**b**) ^{11}B{^{1}H} NMR (128 MHz, d_8-THF, 298K) spectrum of **2**.

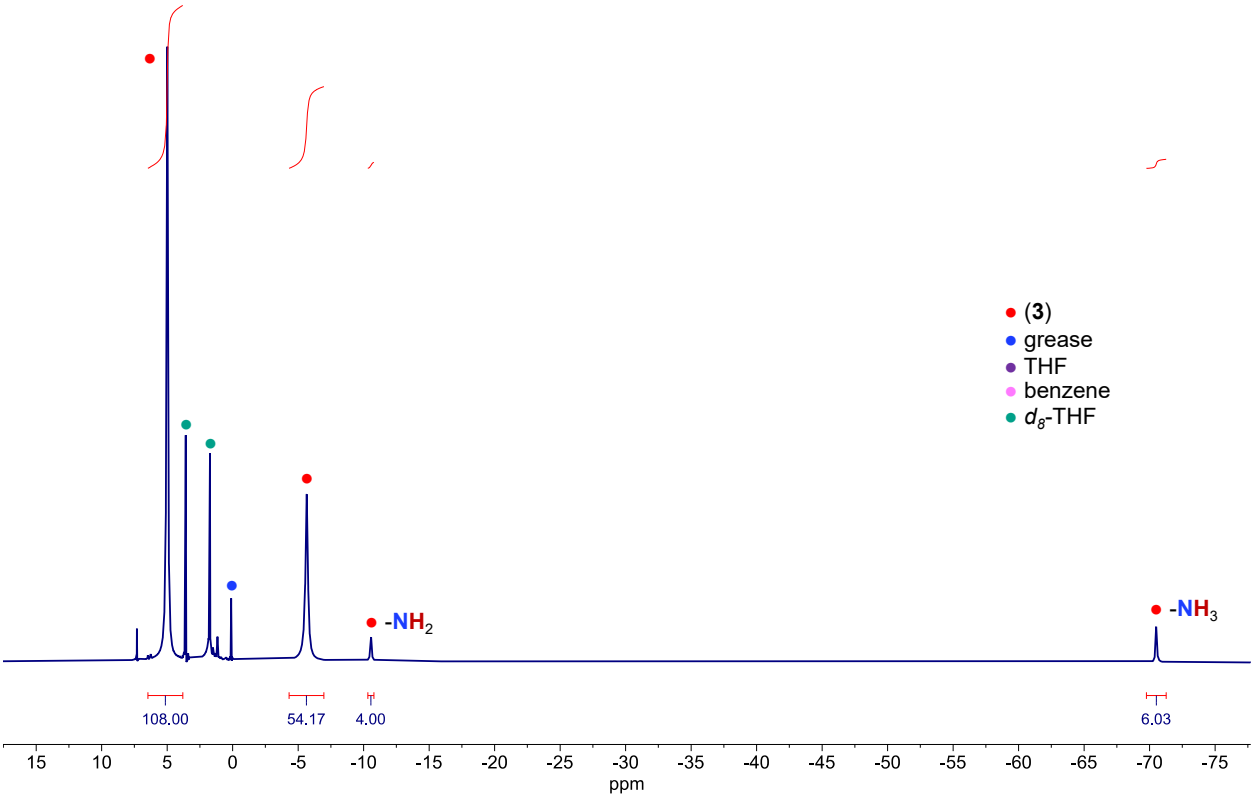

Figure S9. ^{1}H NMR (400 MHz, d_8-THF, 298K) spectrum of [(U^{IV}(OSi(O^{t}Bu)$_3$)$_3$(NH_3))$_2$(μ-NH_2)$_2$], **3**.

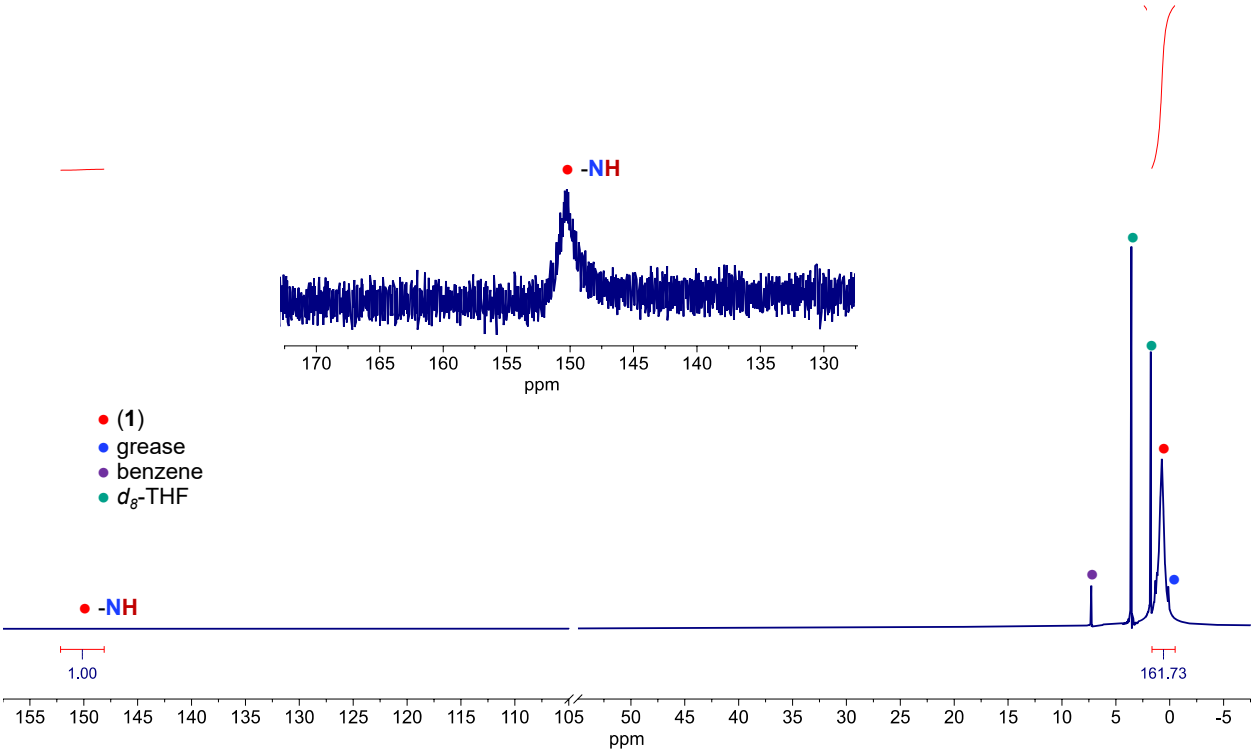

Figure S10. ^{1}H NMR (400 MHz, d_8-THF, 298K) spectrum of $[(U^{IV}(OSi(O^tBu)_3)_3)_2(\mu\text{-}THF)_2(\mu\text{-}NH)]$, **1**.

S5.3. NMR spectra for small molecule reactivity with complex, B.

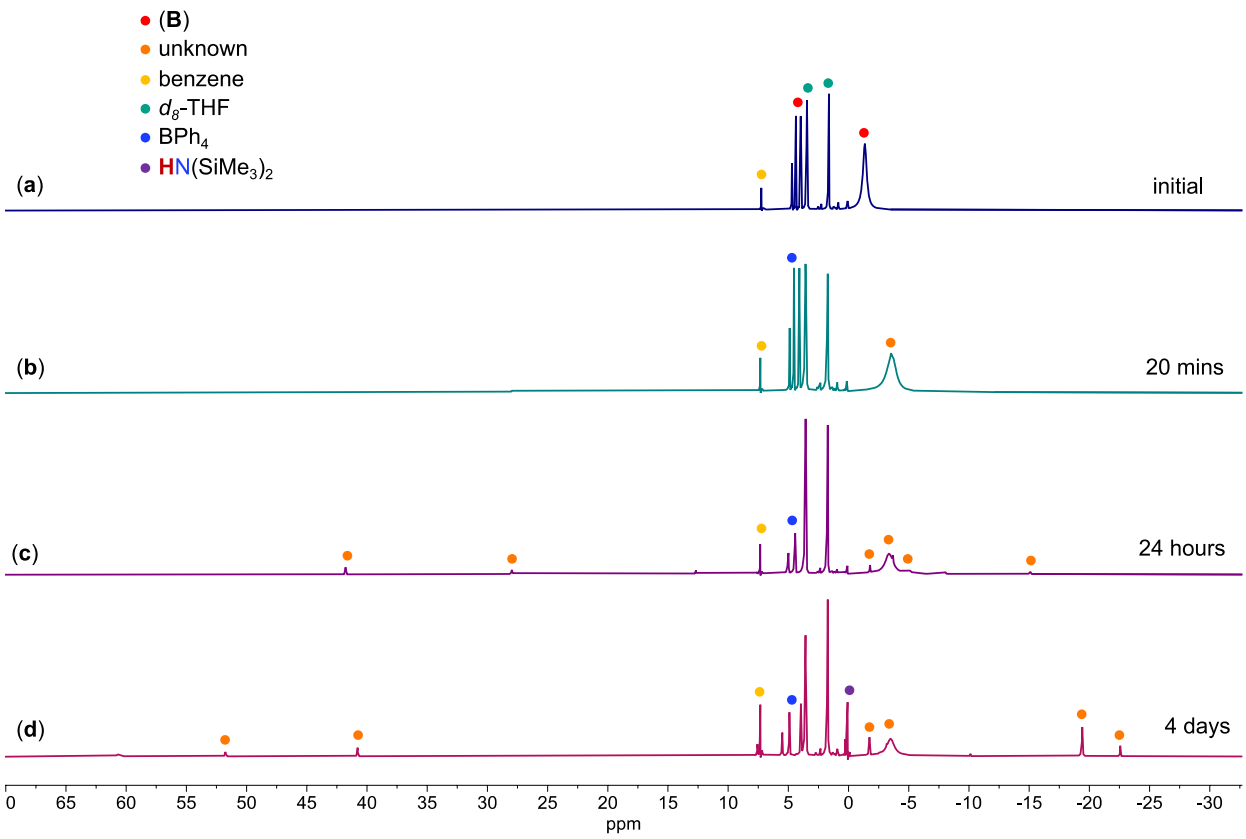

Figure S11. ^{1}H NMR (400 MHz, d_8-THF, 298K) spectrum of **B** in the presence of 2.0 equiv. $^{13}CO_2$ after (**b**) 20 mins (**c**) 24 hours and (**d**) 4 days.

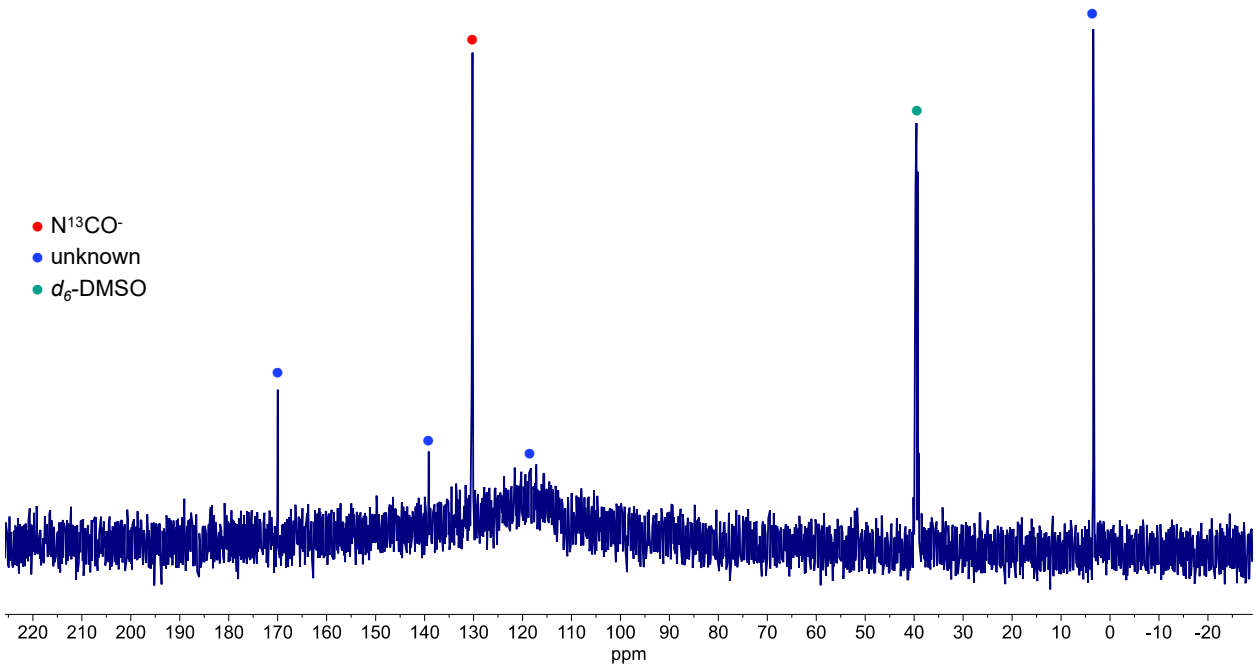

Figure S12. ^{13}C NMR (151 MHz, D_2O, 298K) spectrum after hydrolysis of the reaction mixture with **B** and 2.0 equiv. of $^{13}CO_2$ with a D_2O solution (pD = 12). d_6-DMSO was added as an internal reference.

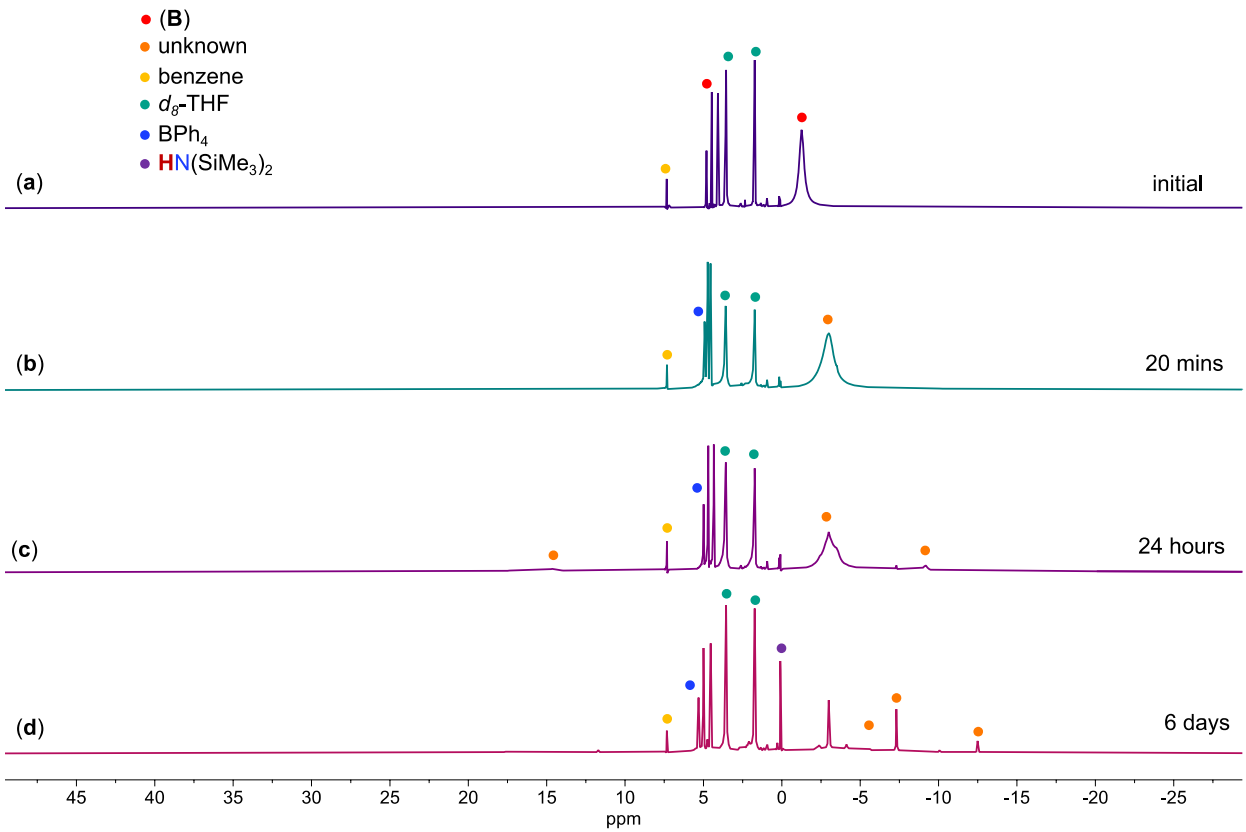

Figure S13. ^{1}H NMR (400 MHz, d_8-THF, 298K) spectrum of **B** in the presence of 2.0 equiv. ^{13}CO after (**b**) 20 mins (**c**) 24 hours and (**d**) 6 days.

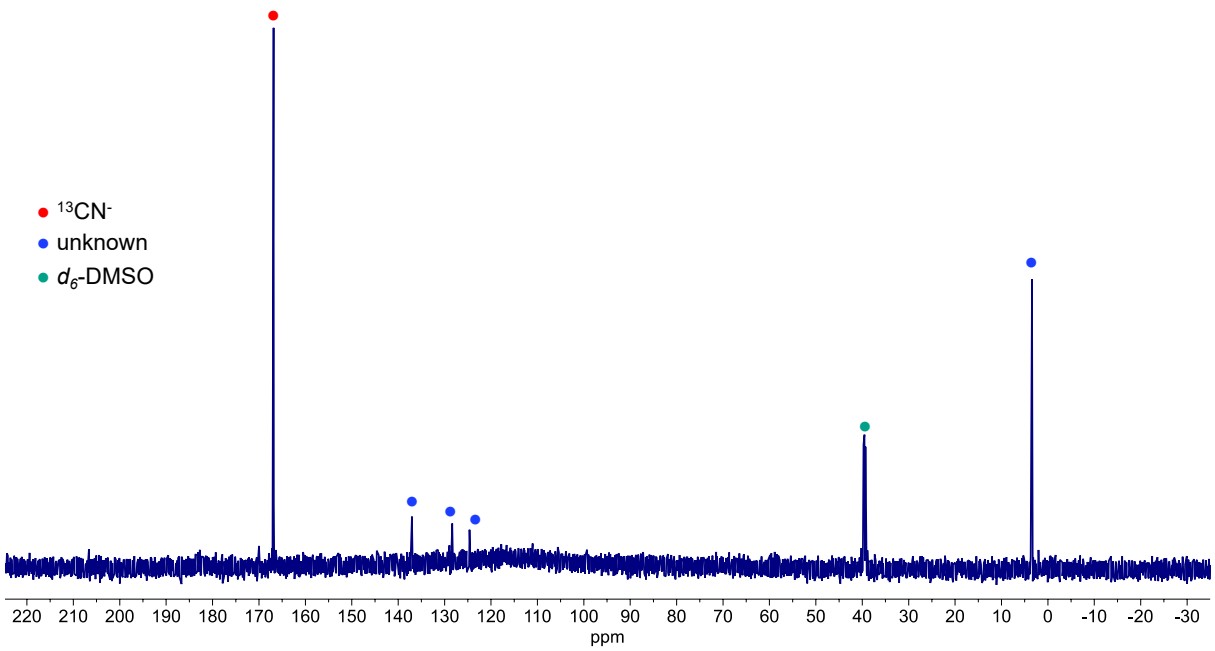

Figure S14. ^{13}C NMR (151 MHz, D_2O, 298K) spectrum after hydrolysis of the reaction mixture with **B** and 2.0 equiv. of ^{13}CO with a D_2O solution (pD = 12). d_6-DMSO was added as an internal reference.

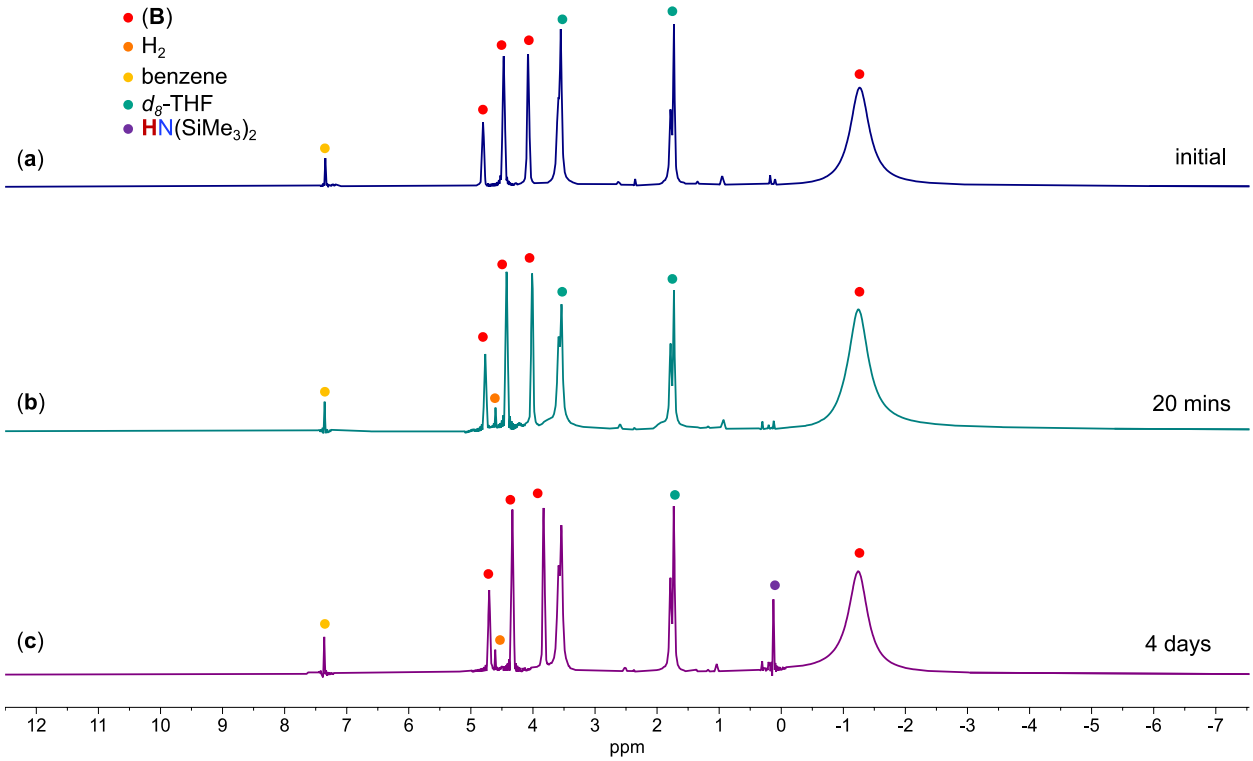

Figure S15. ^{1}H NMR (400 MHz, d_8-THF, 298K) spectrum of **B** in the presence of 1 atm (excess) H_2 after (**b**) 20 mins and (**c**) 4 days, resulting in unreacted starting materials.

S5.4. NMR spectra for protonation studies with complex, B.

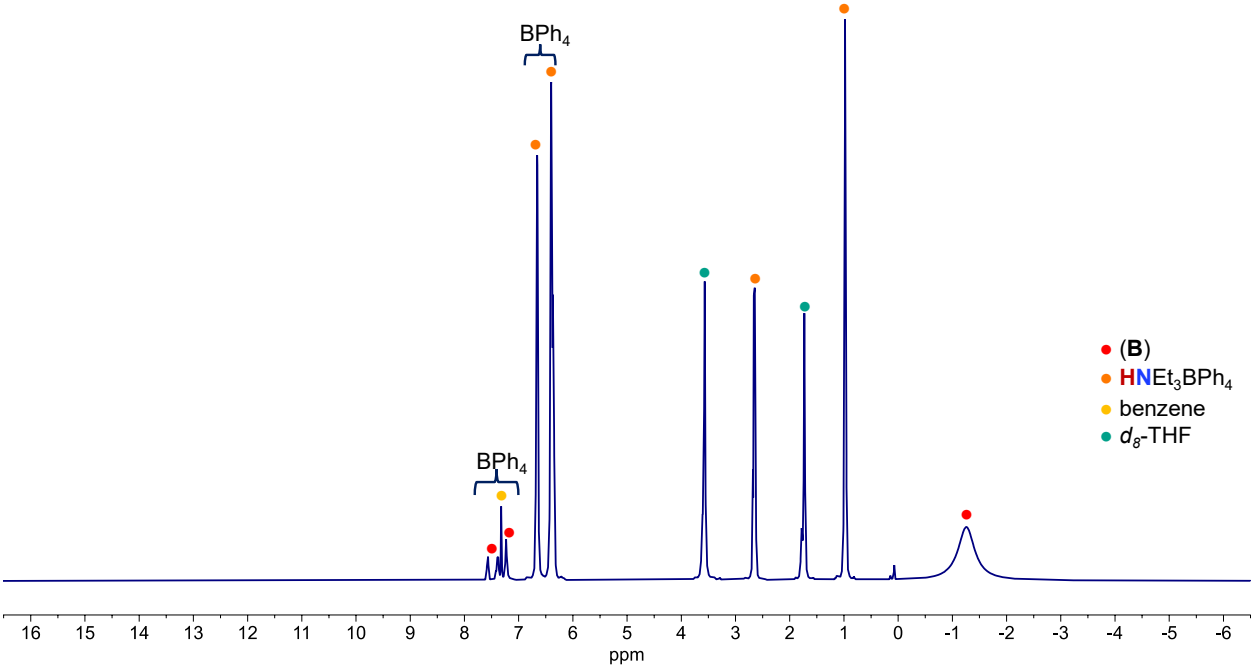

Figure S16. ^{1}H NMR (400 MHz, d_8-THF, 298K) spectra of **B** in the presence of 4.0 equiv. $HNEt_3BPh_4$.

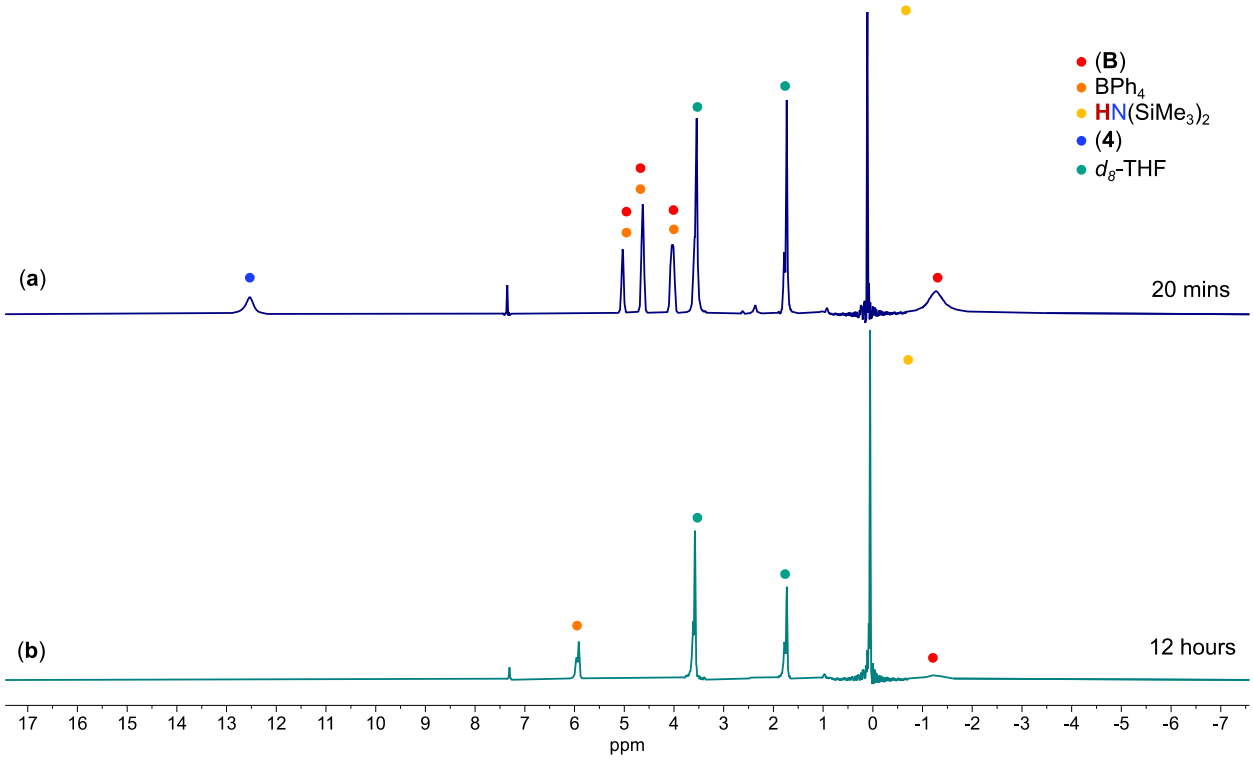

Figure S17. ^{1}H NMR (400 MHz, d_8-THF, 298K) spectra of **B** with 1.0 equiv. NH_4BPh_4 after reacting for (**a**) 20 mins and (**b**) 12 hours.

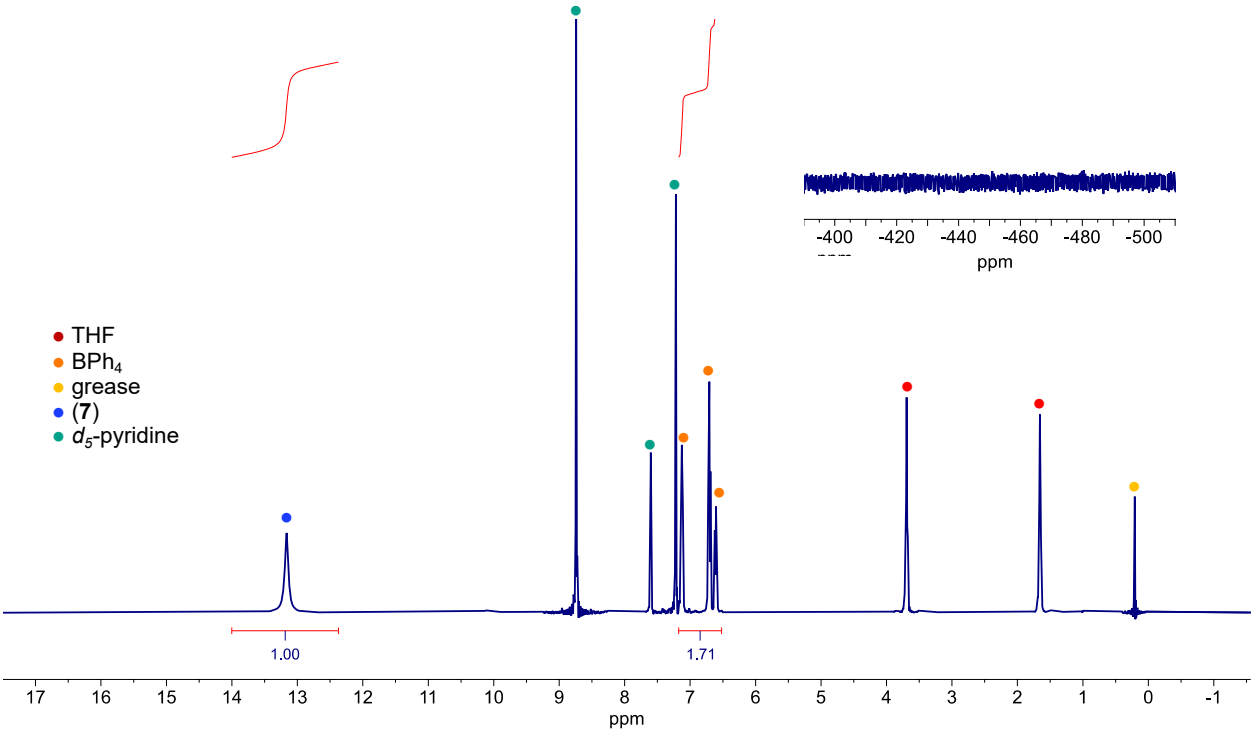

Figure S18. Quantitative ^{1}H NMR (400 MHz, d_5-pyridine, 298K) spectrum of crystals isolated from **B** and 1.0 equiv. NH_4BPh_4 (b, in **Figure S19**). A relaxation delay of 120s were used in order to accurately integrate all species. The following contains a mixture of **B** and an unknown species, based on the relative integrations (1:1.71).

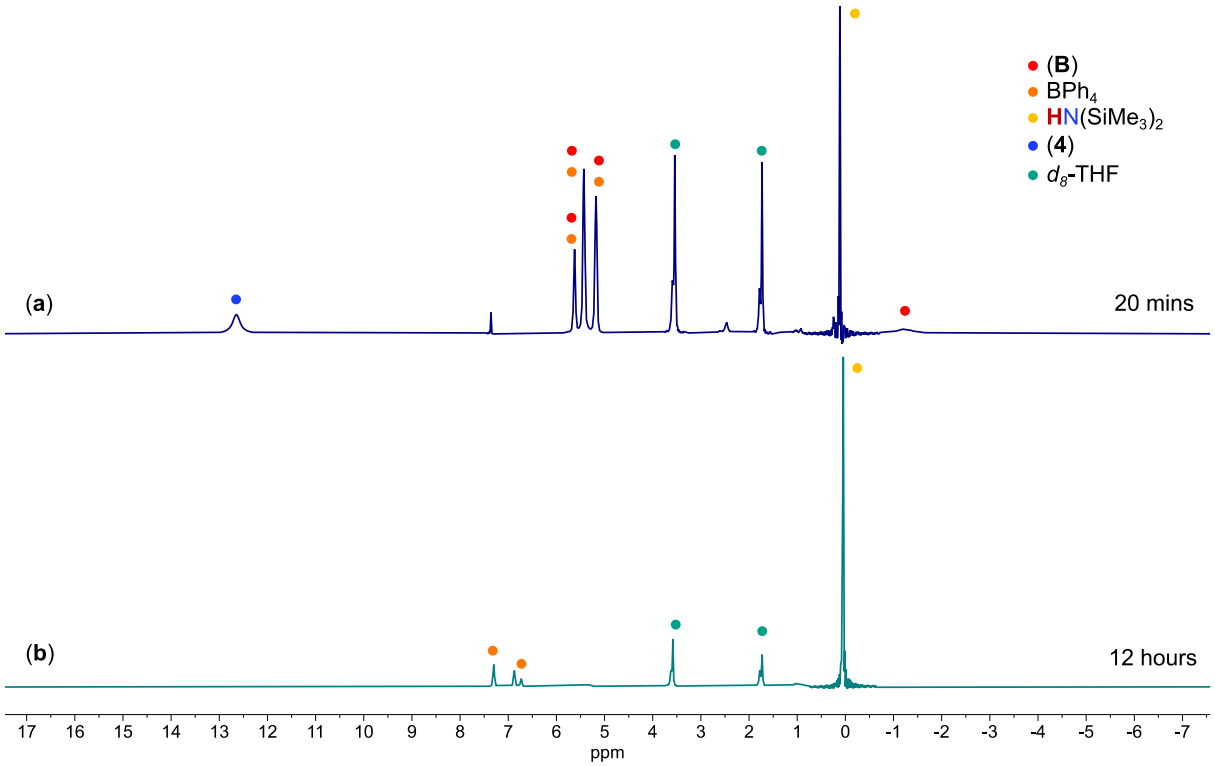

Figure S19. ^{1}H NMR (400 MHz, d_8-THF, 298K) spectra of **B** with 2.0 equiv. NH_4BPh_4 after reacting for (**a**) 20 mins and (**b**) 12 hours.

S5.5. NMR spectra for protonation studies with complex, C.

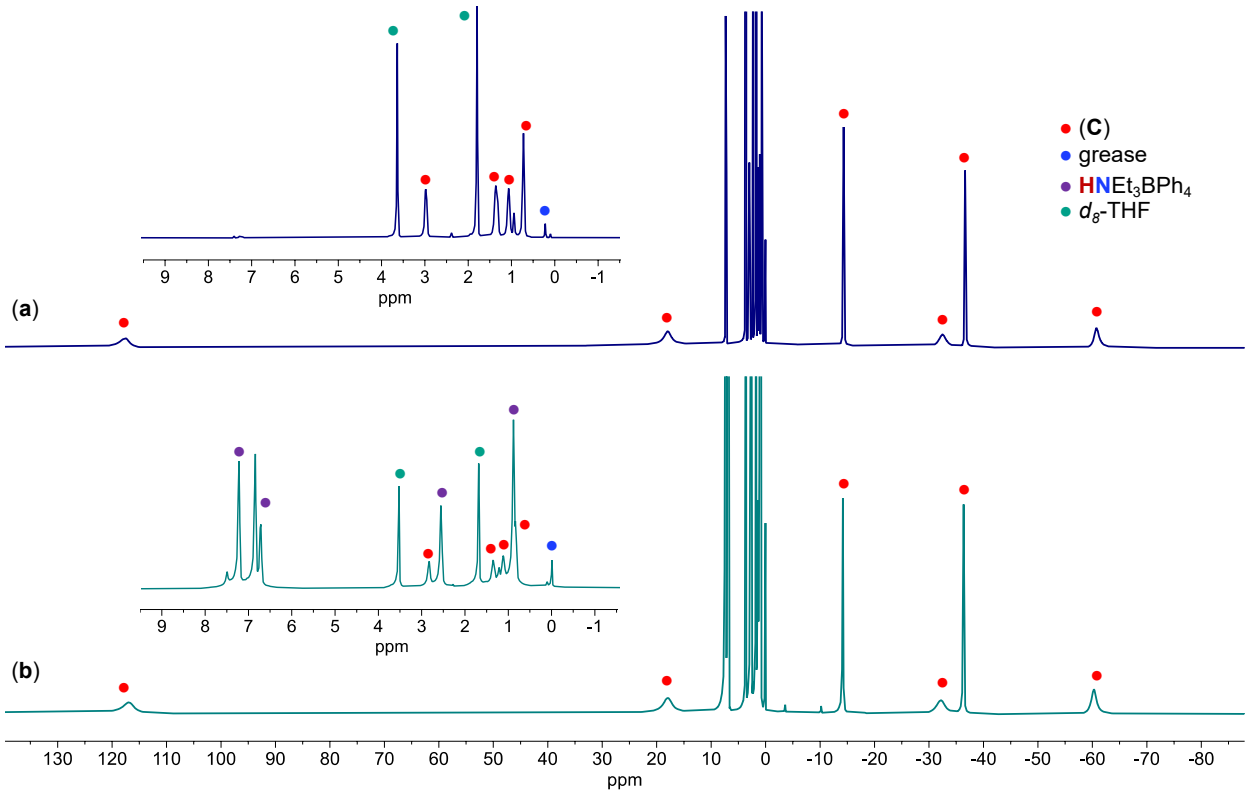

Figure S20. (**a**) ^{1}H NMR (400 MHz, d_8-THF, -60°C) spectrum for complex **C**. (**b**) ^{1}H NMR (400 MHz, d_8-THF, -60°C) spectrum for *in-situ* reaction mixture of complex **C** and 4.0 equiv. of $HNEt_3BPh_4$.

S5.6. NMR spectra for isolated $N(SiMe_3)_2$-containing complexes.

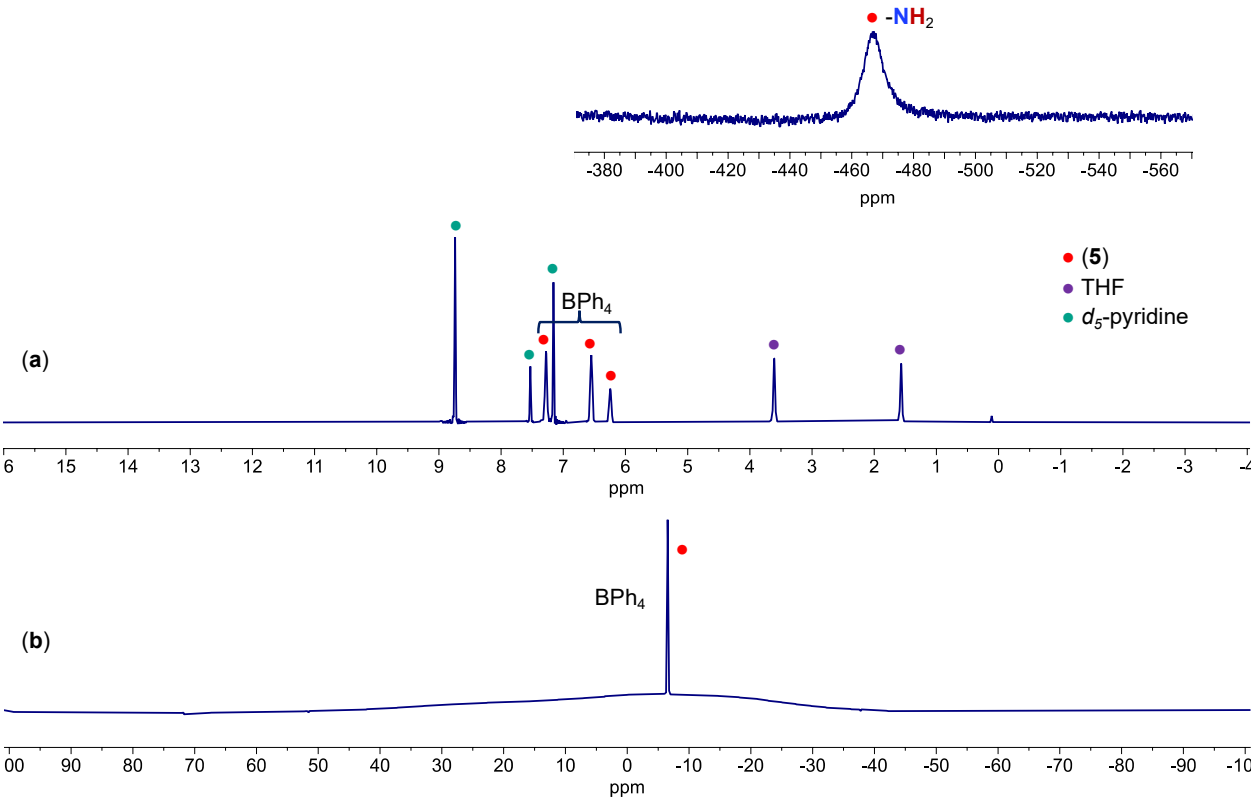

Figure S21. (**a**) ^{1}H NMR (400 MHz, d_5-pyridine, 298K) spectrum of $[(U^{IV}(THF)_4)_2(\mu\text{-}N)(\mu\text{-}NH_2)_2][BPh_4]_3$, **5**. (**b**) $^{11}B\{^{1}H\}$ NMR (128 MHz, d_5-pyridine, 298K) spectrum of **5**.

S5.7. NMR spectra of NH_3 formation from addition of HCl (Et_2O).

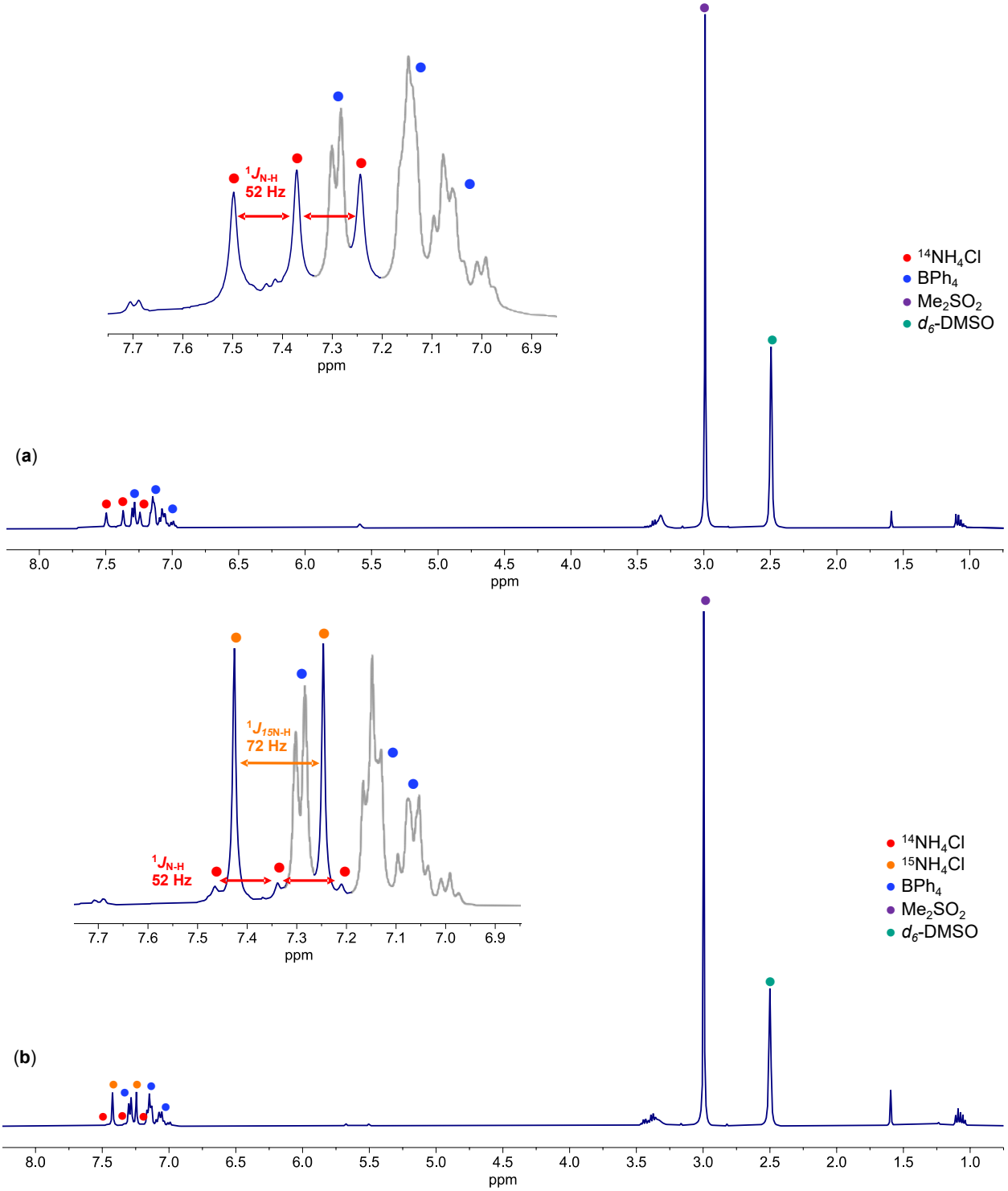

Figure S22. (**a**) ^{1}H NMR (400 MHz, d_6-DMSO, 298K) spectrum of $^{14}NH_4Cl$ formed (95% yield) after addition of **2** and HCl (Et_2O). Me_2SO_2 added as an analytic standard. (**b**) ^{1}H NMR (400 MHz, d_6-DMSO, 298K) spectrum of $^{14/15}NH_4Cl$ formed (97% yield) after addition of **2-$^{14/15}$N** and HCl (Et_2O). Me_2SO_2 added as an analytic standard. All spectra were obtained with a 120s relaxation delay.

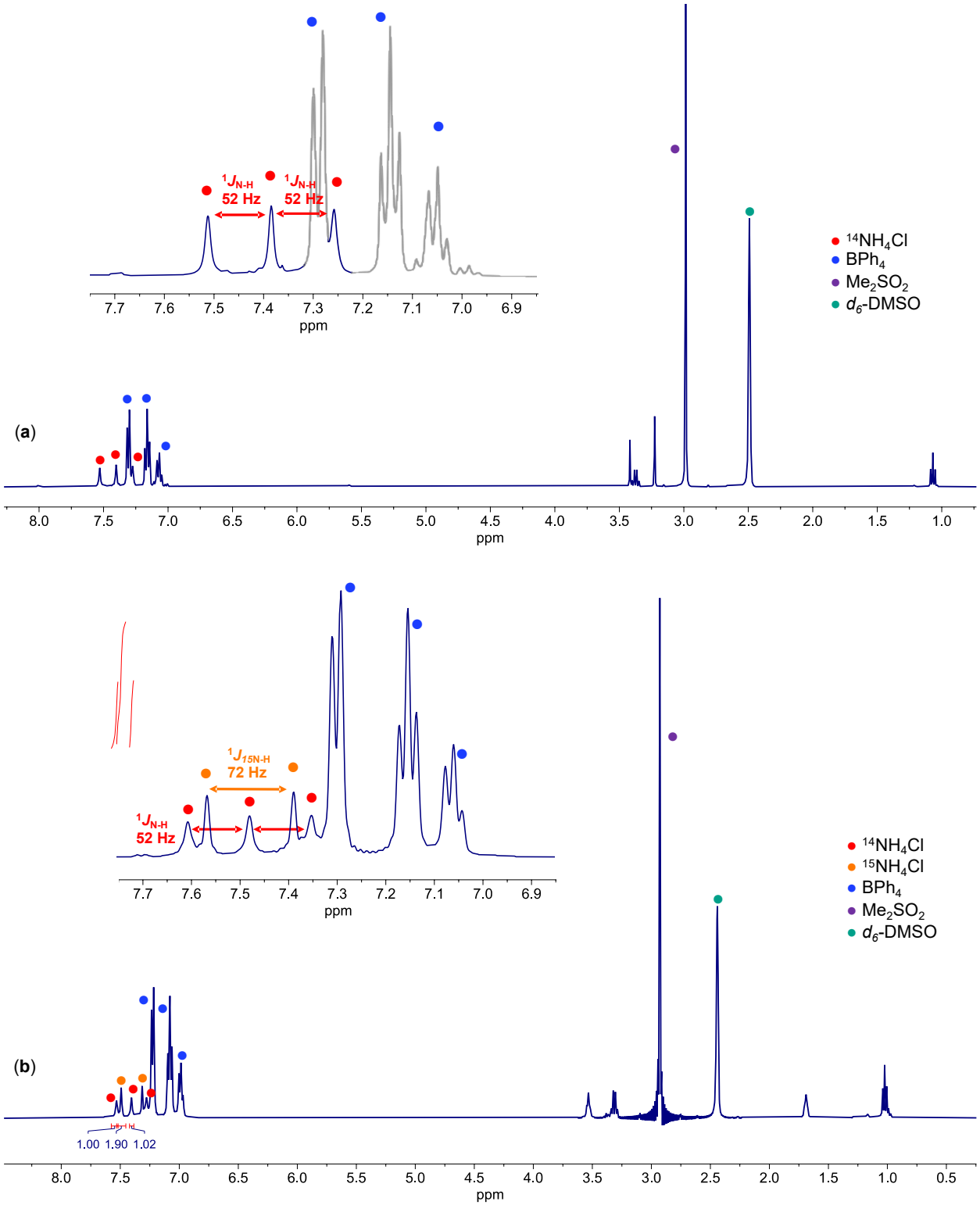

Figure S23. (**a**) ^{1}H NMR (400 MHz, d_6-DMSO, 298K) spectrum of $^{14}NH_4Cl$ formed (95% yield) after addition of **5** and HCl (Et_2O). Me_2SO_2 added as an analytic standard. (**b**) ^{1}H NMR (400 MHz, d_6-DMSO, 298K) spectrum of $^{14/15}NH_4Cl$ formed (92% yield) after addition of **5-$^{14/15}$N** and HCl (Et_2O). Me_2SO_2 added as an analytic standard. All spectra were obtained with a 120s relaxation delay.

S6. Supplementary Figures for X-Ray Crystallography

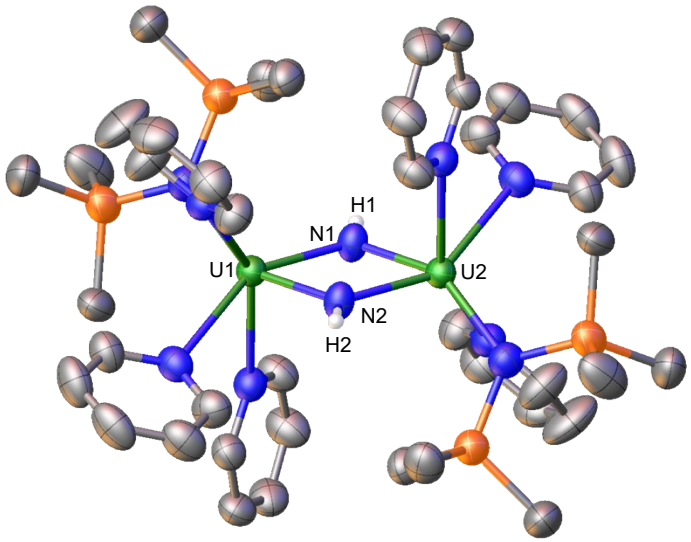

Figure S24. Molecular structure of $[(U^{IV}((N(SiMe_3)_2)(pyridine)_3)_2(\mu\text{-}NH)_2][BPh_4]_2$, **4-pyr**, with thermal ellipsoids drawn at the 50% probability level. Hydrogen atoms, methyl groups, and BPh_4 counterions have been omitted for clarity.

S7. Supplementary Schemes for Proposed Mechanistic Pathways to Complexes 2, 3, 4, and 5.

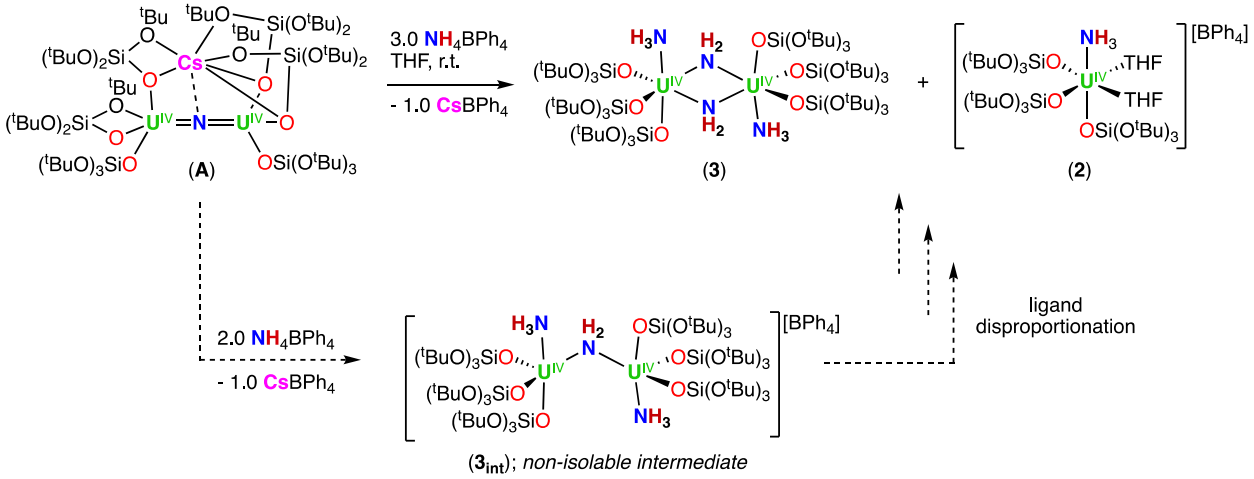

Scheme S1. Proposed reaction mechanism for the formation of complexes **2** and **3**.

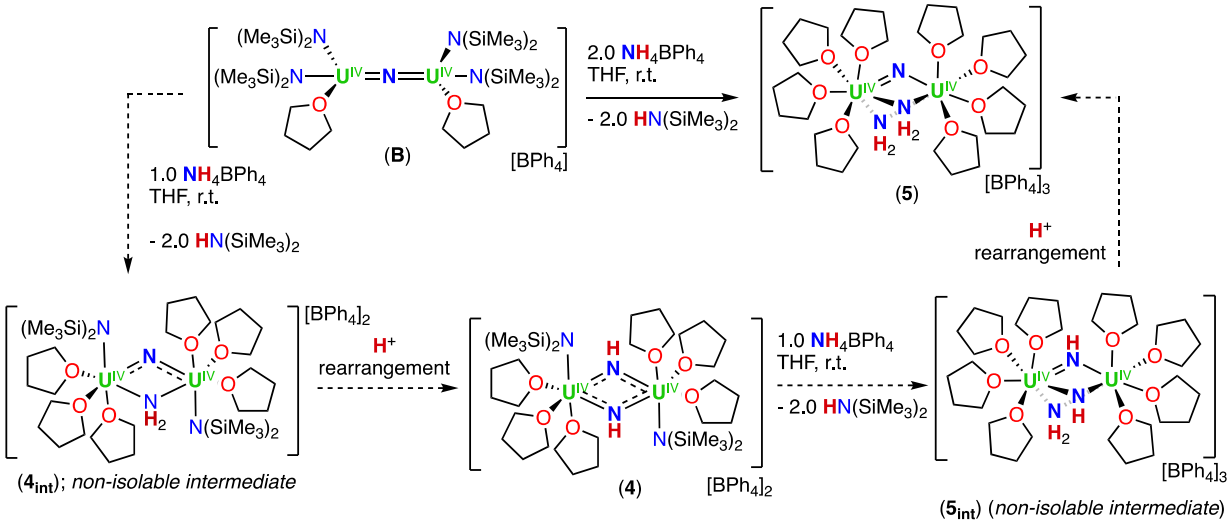

Scheme S2. Proposed reaction mechanism for the formation of complex **5** from **B**, which proceeds via proposed intermediate's $[(U^{IV}((N(SiMe_3)_2)(THF)]_2(\mu\text{-}NH_2)(\mu\text{-}N)[BPh_4]_2$, $\mathbf{4_{int}}$, $[(U^{IV}((N(SiMe_3)_2)(THF)_3)_2(\mu\text{-}NH)_2][BPh_4]_2$, **4,** and $[(U^{IV}(THF)_4)_2(\mu\text{-}NH)_2(\mu\text{-}NH_2)][BPh_4]_3$, $\mathbf{5_{int}}$.

S8. References

1. C. Camp, J. Pécaut and M. Mazzanti, *J. Am. Chem. Soc.*, 2013, **135**, 12101-12111.
2. C. T. Palumbo, R. Scopelliti, I. Zivkovic and M. Mazzanti, *J. Am. Chem. Soc.*, 2020, **142**, 3149-3157.
3. C. T. Palumbo, L. Barluzzi, R. Scopelliti, I. Zivkovic, A. Fabrizio, C. Corminboeuf and M. Mazzanti, *Chem. Sci.*, 2019, **10**, 8840-8849.
4. C. Boisson, J. C. Berthet, M. Ephritikhine, M. Lance and M. Nierlich, *J. Organomet. Chem.*, 1997, **533**, 7-11.
5. *CrysAlis*^{Pro}, Rigaku Oxford Diffraction, release 1.171.41.113a, 2021.
6. G. M. Sheldrick, *Acta Crystallogr. A*, 2015, **A71**, 3-8.
7. G. M. Sheldrick, *Acta Crystallogr. C*, 2015, **C71**, 3-8.
8. A. Spek, *Acta Crystallogr. D*, 2009, **65**, 148-155.